

Review

Nanoadsorbants for the Removal of Heavy Metals from Contaminated Water: Current Scenario and Future Directions

Rohit Kumar, Protima Rauwel  and Erwan Rauwel * 

Institute of Technology, Estonian University of Life Sciences, Kreutzwaldi 56/1, 51014 Tartu, Estonia; rohit.kumar@student.emu.ee (R.K.); protima.rauwel@emu.ee (P.R.)

* Correspondence: erwan.rauwel@emu.ee

Abstract: Heavy metal pollution of aquatic media has grown significantly over the past few decades. Therefore, a number of physical, chemical, biological, and electrochemical technologies are being employed to tackle this problem. However, they possess various inescapable shortcomings curbing their utilization at a commercial scale. In this regard, nanotechnology has provided efficient and cost-effective solutions for the extraction of heavy metals from water. This review will provide a detailed overview on the efficiency and applicability of various adsorbents, i.e., carbon nanotubes, graphene, silica, zero-valent iron, and magnetic nanoparticles for scavenging metallic ions. These nanoparticles exhibit potential to be used in extracting a variety of toxic metals. Recently, nanomaterial-assisted bio-electrochemical removal of heavy metals has also emerged. To that end, various nanoparticle-based electrodes are being developed, offering more efficient, cost-effective, ecofriendly, and sustainable options. In addition, the promising perspectives of nanomaterials in environmental applications are also discussed in this paper and potential directions for future works are suggested.



Citation: Kumar, R.; Rauwel, P.; Rauwel, E. Nanoadsorbants for the Removal of Heavy Metals from Contaminated Water: Current Scenario and Future Directions. *Processes* **2021**, *9*, 1379. <https://doi.org/10.3390/pr9081379>

Academic Editors: Monika Wawrzekiewicz and Anna Wołowicz

Received: 18 June 2021
Accepted: 30 July 2021
Published: 6 August 2021

Publisher's Note: MDPI stays neutral with regard to jurisdictional claims in published maps and institutional affiliations.



Copyright: © 2021 by the authors. Licensee MDPI, Basel, Switzerland. This article is an open access article distributed under the terms and conditions of the Creative Commons Attribution (CC BY) license (<https://creativecommons.org/licenses/by/4.0/>).

Keywords: nanomaterials; heavy metals; remediation; bioelectrochemical systems; wastewater; adsorption; nanocomposites

1. Introduction

Even though 70% of the Earth's surface is composed of water, freshwater resources are rapidly dwindling. The latter accounts for approximately 1% of total water bodies. In addition, the contamination of these aqueous resources with a broad range of pollutants due to rapid industrialization and lifestyle changes has further reduced the availability of clean fresh water sources. In particular, mining, volcanic eruptions, farming, and excessive dumping of hazardous chemicals has resulted in a significant invasion of organic compounds, pharmaceuticals, customer care products, pathogens, and heavy metals into water reservoirs [1]. Among the persistent pollutants, the existence of heavy metals in water is considered as a prime global concern due to their considerable role in environmental degradation [2,3].

In general, heavy metals (HM) can be defined as a group of transition metals, metalloids, actinides, and lanthanides with a density greater than 4000 kg/m³, and can be further categorized into the groups of essential and non-essential metals [4]. Under both categories, they are heavily involved in a vast number of industries and crafts and are an essential part of various biological processes/reactions [5]. However, long-term, and sometimes short-term, exposure to them, even in trace amounts, can lead to serious health implications [6]. The most commonly-encountered heavy metals in water include Pb, Cd, Cr, Co, As, Zn, Hg, and Ni. They are considered as particularly problematic due to their non-biodegradability and bioaccumulation behavior when ingested; thus, they are listed in the Environmental Protection Agency's list of priority pollutants [7,8]. More specifically, the intake of Cd, Pb, Hg, Cr, and As beyond the standard limits can give rise to serious health implications such as bone defects, increased blood pressure, lung cancer, nervous system damage, neurological depositions, gastrointestinal disorders, and many more significant

diseases [9–11]. Therefore, considering the complex chemistry and carcinogenicity of HM, there is an urgent need to develop appropriate methods for their extraction from water sources. Several physical, chemical, biological, and electrochemical methods, along with their combinations, which have been studied and researched for HM removal over the past few decades are briefly summarized in Table 1.

Table 1. Conventional approaches for the remediation of heavy metals and their associated advantages and disadvantages.

Technology	Advantages	Disadvantages	References
Physical			
1. Membrane separation	1. Very effective in treatment of a variety of metals.	1. Production of hazardous by-products.	[12,13]
2. Adsorption/Physiosorption	2. Easily applicable	2. Energy intensive	
3. Filtration	3. Economically acceptable		
4. Sedimentation			
Chemical			
1. Adsorption/Chemisorption	1. Easy to apply and very effective.	1. Applicable at small scale.	[14–16]
2. Ion-exchange	2. Applicable to a broad range of inorganic/organic pollutants.	2. Formation of more toxic chemical by-products.	
3. Chemical precipitation			
4. Flocculation/Coagulation			
Biological (Microbes assisted remediation)	1. Environmental-friendly and cost effective. 2. Applicable at large scale. 3. Less disruptive.	1. Well-defined growth conditions required for microbes. 2. Slow process. 3. Continuous monitoring required.	[17–19]
Electrochemical	1. Very effective and efficient in treating a vast variety of pollutants including heavy metals. 2. Production of energy.	1. Energy and cost intensive process. 2. Applicable at small scale. 3. Chemically intensive process.	[20–22]

The conventional technologies summarized in Table 1 are effective but present some unavoidable drawbacks, such as high costs, energy intensiveness, tediousness, low efficiency, metal specificity, and unsustainability, thereby rendering them ineffective in meeting environmental standards and, in turn, too difficult to implement at the industrial scale [23]. Therefore, considering the negative impacts of HM on human health and the environment, one deems it necessary to introduce a cost-effective, environmental-friendly and efficient processes for the removal of HM from the contaminated water. Adsorption is a mass transfer process, where the adsorbate molecules are attracted to the surface of an adsorbent, resulting in either a physical or chemical interaction. It is one of the most favored processes in the water treatment industry, especially due to the regenerative capacity of the adsorbents [24]. Therefore, among the technologies reviewed, adsorption is considered the most efficient, safe, and technically feasible process due to its facile operation and higher efficiency [25]. In fact, the adsorption capacity varies with the type of adsorbent. Generally, activated carbon based adsorbents are widely used for the removal of heavy metals but due to their clogging, inability to recover them from the treated water, waste generation, and biofouling, they are ineffective for large scale applications [26,27]. Therefore, the search for new and effective adsorbent materials has always been an active field of research [28]. Nanomaterials, due to their nanoscale dimensions (ranging from 1–100 nm), show some unique physical, chemical, and biological properties. These properties result in the modification of their structure and specific surfaces [29]. Different kinds of nano-adsorbents and nanocomposites have been extensively researched and are used for the treatment of organic dyes, inorganic compounds, heavy metals, and other micropollutants (customer-care products, biocides and hormone active substances) from water/wastewater [30]. This

manuscript will firstly provide a review of the different types of nanomaterial-based adsorbents used for heavy metal extraction. The main focus of this review is to provide a basic insight of the conventional nanomaterials used (CNT-GO, silica-based, ZVI) and show how magnetic NP exhibit a significant advantage over these nanomaterials. However, the main disadvantages of magnetic nanomaterials are also considered and discussed. The possible combination of these nanomaterials with existing technology is then discussed and the last part of the review particularly discusses the industrially active adsorbents and how the electro-chemical technologies combined with nanomaterials can provide a sustainable, cost effective, and ecofriendly approach in the future. The second part of the review will concentrate on the nanomaterial assisted bioelectrochemical remediation of metallic ions with an emphasis on the current developments and next generation nanoadsorbents. Several studies suggest that there are improvements in the metal reduction efficiency when nanomaterials are introduced in bioelectrochemical systems (BES).

2. Nanomaterials Applied for the Removal of Metallic Ions from Water

Nanomaterials (NM), due to properties such as high specific surface, porosity, surface functionalities, and ion binding capabilities, have been widely researched over the past two decades in water and wastewater treatment applications. In fact, they also show a high potential in the removal of metallic ions even in trace amounts [31,32]. Nanomaterials are classified into different categories, i.e., carbon based, silica based, metal and metal oxide nanoparticles, including zero-valent iron (ZVI), iron-oxide based magnetic nanomaterials, and nanocomposites, as shown in Figure 1. There are several factors, such as concentration of adsorbent, contact time, and flow rate, that control the adsorption process of metallic ions. However, the concentration of nanoparticles (adsorbent) plays a crucial role in the removal process. Some studies suggest an increase in the removal efficiency when the adsorbent dosage increases, whereas some studies report a decrease in the removal when the adsorbent concentration increases due to a possible agglomeration process. For example, Lei et al. reported a decrease in the adsorption capacity of Cd^{2+} ions when the amount of Dopamine-Modified Magnetic Nano-Adsorbent was increased from 10–50 mg [33]. The probable reason mentioned was the agglomeration of the adsorbent at higher concentrations which inhibits the adsorption process due to surface adsorption decrease. In fact, in another study an increase in the removal efficiency of Cd^{2+} ions (83% to 89%) was observed when the concentration of gas industry-based adsorbent was increased from 0.25–1.25 g/100 ML [34]. In gas phase, it was found that no agglomeration takes place, so the adsorption only depends on the amount of adsorbent added. Based on these studies, it can be concluded that the concentration of adsorbent affects the removal process, but it depends on the nature and chemical properties of the adsorbent itself, suggesting that either an increase or decrease in the removal will occur. However, higher and lower volumes of NP with equal concentration will lead to the same results.

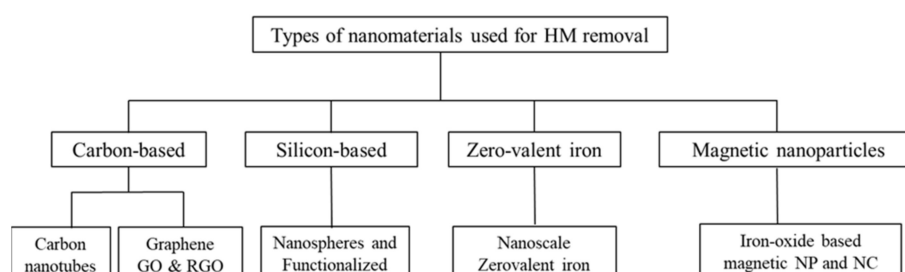


Figure 1. Nanomaterials for heavy metal remediation in aqueous media.

2.1. Carbon Based Nanomaterials

Carbon-based NM, such as carbon nanotubes, Fullerenes, activated carbon, graphene, and graphene oxide, have been widely used in energy storage, sensors, electronics, water purification, drug delivery, and disease diagnosis [35]. In addition, their unique properties

also allow the removal of both organic and inorganic pollutants, making them a promising alternative for treating wastewater. They are therefore considered as one of the most promising adsorbents for metallic pollutants [36,37].

2.1.1. Carbon Nanotubes

Carbon nanotube (CNT) adsorbents are widely employed for metallic pollutant extraction [38]. They are broadly classified into single walled carbon nanotubes (SWCNT) and multi-walled carbon nanotubes (MWCNT), and both are extensively tested for the removal of heavy metals [39–41]. In the case of CNT, the adsorption process is usually controlled by four possible active sites: (i) the hollow interior of individual CNT designated as internal sites; (ii) the interstitial channels between CNT in the stacks; (iii) the grooves between adjacent CNT; and (iv) the external surface of individual CNT [42,43] (Figure 2). The sites of interstitial channels and grooves are responsible for initializing the process of adsorption, which is then followed by the adsorption of the contaminants on the external walls and the accumulation of molecules on internal axial sites. From a kinetic point of view, internal sites are more inclined to acquire the equilibrium state than the external sites under the same conditions. Therefore, increasing the binding sites on the CNT surface can undoubtedly enhance the saturation capability and kinetic rate. The applicability of CNT in wastewater treatment is dependent on several factors including the cost to complexity of CNT functionalization, the necessity for solid and liquid segregation, the type of wastewater, and the recycling cost and efficiency.

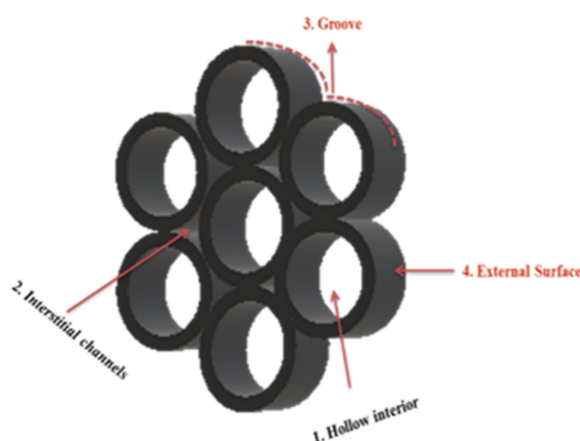


Figure 2. Possible active adsorption sites on the carbon nanotubes (CNT) surface.

Many studies have been performed on CNT-based composites for the remediation of trace elements in water such as heavy metal ions (See Table 2).

Table 2. Summary of the types of CNT used for the removal of different metallic ions.

Type of CNT	Target Metal/s	Initial Concentration (mg/L)	%Removal Efficiency	References
SWCNT	Hg ²⁺	(1–2000) mg/L	4.16%	[44]
MSWCNT-CoS	Hg ²⁺	(1–2000) mg/L	166.6%	[39]
MWCNT-SH	Hg ²⁺	10 mg/L	15.15%	[45]
SWCNTs-polysulfone nanocomposite-based membrane	Pb ²⁺ , As ³⁺	1 mg/L	94.2%, 87.6%	[46]
MWCNT-COOH functionalized nanotube	Pb ²⁺	(10–100) mg/L	99.1%	[47]
Acidified MWCNT	Pb ²⁺ , Cu ²⁺ , Ni ²⁺	100 mg/L	93%, 78%, 83%	[48]
MWCNT	Mn ⁷⁺	(50–800) mg/L	71.5%	[49]
MWCNTs	Cd ²⁺	100 mg/L	10.7% (pH = 2) 94.2% (pH = 7) 100% (pH = 10)	[48]
Oxidized MWCNT	Cu ²⁺	100 mg/L	78%	[48]
MWCNT	Fe ²⁺	200 mg/L	52%	[49]
Oxidized MWCNT	Ni ²⁺	100 mg/L	83%	[48]

The adsorption affinity of CNT towards HM ions varies as a function of the ionic radius of metallic ions, electronegativity of metals, and solubility of metal hydroxides. These factors play an important role in understanding the interaction between metal ions and adsorbents. The ionic radii, in increasing order, are Pb²⁺ (120 pm) > Sr²⁺ > Ca²⁺ (100 pm) > Cd²⁺ (99 pm) > Mn²⁺ (80 pm) > Cu²⁺ (77 pm) > Zn²⁺ (74 pm) and Co²⁺ (72 pm) > Ni²⁺ (69 pm) [50]. This suggests that higher ionic radii generate higher steric overcrowding, which in turn, lowers the maximum adsorption capacity. For example, Brasquet et al. investigated the adsorption affinities of Pb²⁺ and Cu²⁺ towards activated carbon cloth and established a higher adsorption capacity for Cu²⁺. The larger ionic radius of Pb²⁺ induces a quicker saturation of the adsorption sites, probably due to overcrowding of Pb²⁺ ions on the adsorbent surface [51]. On the other hand, the surface adsorption available for the Cu²⁺ ions are larger, due to its smaller ionic radius, resulting in its higher maximum adsorption capacity. The metal ions that exhibit higher electronegativity will have a stronger adsorption capacity towards the negatively charged sites on the CNT surface. The adsorption capacities of Pb²⁺ and Cu²⁺ were investigated in regard to MWCNT and since Cu²⁺ has a lower electronegativity (1.99) than Pb²⁺ (2.33), it therefore leads to weaker interactions towards the CNT surface and maximum adsorption levels of Cu²⁺ decreased by approximately 12% in comparison with Pb²⁺ [52]. Various functionalized and pure CNT have been extensively investigated, and authors report an efficient extraction of heavy metals from contaminated water (discussed in Table 2). They present high adsorption efficiencies in comparison with activated carbon, which is widely used in various water treatment industries. Moreover, their regeneration and reuse provide a special benefit over other conventional adsorbents such as activated carbon, clays, and biosorbents [53]. Besides their notable potential for HM extraction, there are some unavoidable shortcomings associated with them. One of the main problems of using CNT is associated with their agglomeration or bundling resulting in a lower specific surface for adsorption. Moreover, when it comes to their applicability at an industrial scale, their attachment to filters should be strong enough to prevent their release into treated waters [54].

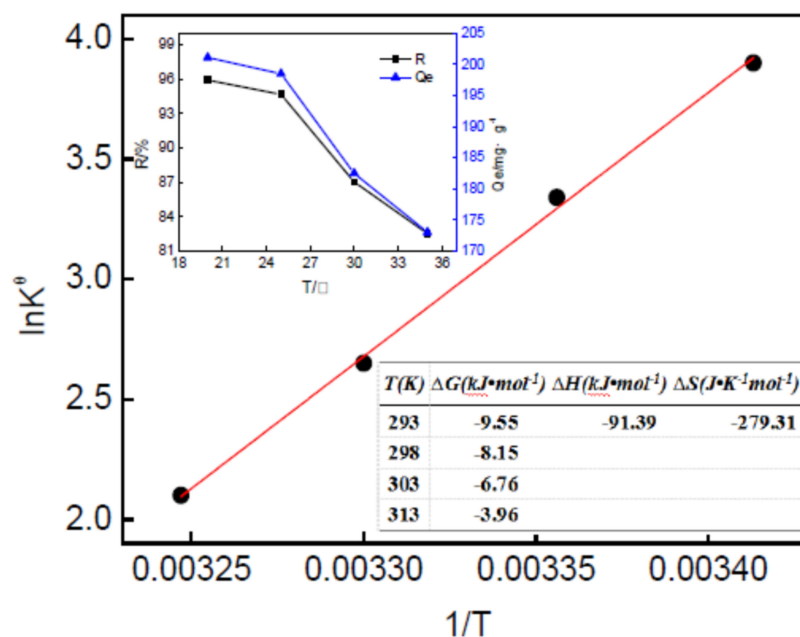
2.1.2. Graphene Based Adsorbents

Graphene is another carbon-based material with high adsorption capabilities in removing HM from wastewater [55–57]. It is a 2D material in which carbon atoms are

arranged in a hexagonal, honeycomb lattice. Graphene can be classified into two major forms, graphene oxide (GO), the oxidized form, and reduced graphene oxide (RGO); the latter shows potential towards remediation of various environmental pollutants [58]. In fact, the availability of several functional groups, i.e., hydroxyl, carboxyl, and epoxide on the surfaces of GO and RGO serve as the active sites for the removal of metallic ions from water [59,60]. The functional groups, e.g., $-\text{CH}(\text{O})\text{CH}-$, $-\text{OH}$, and $-\text{COOH}$ have high negative charge densities along with hydrophilic characteristics, which promote their interactions with positively charged metal ions in order to facilitate the extraction mechanisms [61]. Graphene and GO/RGO-based materials have been extensively studied and are reported to have excellent properties for heavy metal ion extraction from water/wastewater (Table 3) [61]. For example, few-layered graphene oxide nanosheets were investigated for the adsorption of Cd^{2+} and Co^{2+} from the contaminated water in batch mode [62]. This study highlighted a strong influence of pH and the presence of humic acid in adsorption of Cd^{2+} and Co^{2+} . However, the maximum adsorption capacities of Cd^{2+} and Co^{2+} were found to be 106.3 mg/g and 68.2 mg/g respectively. Wang et al. studied different factors including pH, the dosage of the adsorbent, contact time, temperature, and competing ions on the adsorption performance of GO for the removal of zinc ions and observed an adsorption capacity of 246 mg/g of Zn^{2+} [63]. The removal of Pb^{2+} ions from water was investigated using a nanocomposite of Fe_3O_4 and reduced graphene oxide ($\text{Fe}_3\text{O}_4@\text{RGO}$). This study showed an adsorption capacity of 373.14 mg/g with an initial Pb^{2+} concentration of 97.68 mg/L [64]. Figure 3 shows different thermodynamic parameter values represented by the Van't Hoff curve at room temperature, confirming that the adsorption is a spontaneous exothermic process with a relatively low entropy. The absolute value of ΔH was found to be higher than $20 \text{ kJ}\cdot\text{mol}^{-1}$, implying a strong chemical interaction between adsorbent and adsorbate. The experimental data fitted Temkin's model which assumes the adsorption heat of all the molecules in the layer decreases linearly with coverage due to chemical interactions between adsorbent and adsorbate, and that the adsorption is characterized by a uniform distribution of the binding energies, up to a maximum binding energy. Based on this assumption, they concluded that monolayer chemisorption is the main adsorption mechanism. In fact, in addition to the latter, liquid film diffusion was also found to have interplay with this mechanism. Porous graphene was designed and studied for the adsorption of As^{3+} from water [65]. This synthesized adsorbent showed an adsorption capacity >90% and retained its water treatment properties even after regeneration and recycling. However, porous graphene applied to the cleaning of real wastewater that contains various competing elements poses a notable disadvantage in the case of large-scale applications. The authors concluded that monolayer chemisorption takes place during the extraction process. Functionalized reduced graphene oxide with 4-sulfophenylazo (RGOs) was studied for the removal of heavy metal ions from aqueous solution. The nanomaterial designed showed a maximum adsorption capacity of 689 mg/g, 59 mg/g, 66 mg/g, 267 mg/g, and 191 mg/g for the Pb^{2+} , Cu^{2+} , Ni^{2+} , Cd^{2+} , and Cr^{3+} respectively [66]. The adsorption of RGOs for Pb^{2+} , Cd^{2+} and Cr^{3+} was ascribed to coordination reaction of N atoms with heavy metal ions. Awad et al. found a significant increase in the adsorption capacity of Hg^{2+} onto the modified GO surface with COOH groups (24 mg/g to 122 mg/g), which suggests stronger interactions of Hg^{2+} ions towards negatively charged COOH groups [67].

Table 3. Graphene derived nanoparticles for the removal of heavy metals.

Adsorbate	Target Metal	Initial Concentration	Removal %	References
Tea polyphenols—rGO-ZnO	Pb ²⁺	20 mg/L	98.9%	[68]
Porous Graphene	As ³⁺	130 mg/L	>90%	[65]
rGO-Fe ₃ O ₄	Pb ²⁺	20 mg/L	37.314%	[64]
rGO-Sulfophenylazo	Cu ²⁺ , Ni ²⁺	40 mg/L	5.9 %, 6.6 %	[66]
GO embedded calcium alginate (GOCA) beads	Pb ²⁺ , Cd ²⁺ , Hg ²⁺	50 mg/L	60.2%, 18.1%, 37.4%	[69]
rGO-Sulfophenylazo	Cd ²⁺	40 mg/L	26.7%	[66]
GO-alpha cyclodextrin-polypyrrole	Cr ⁶⁺	100–700 mg/L	66.67%	[70]
rGO-Sulfophenylazo	Cr ³⁺	40 mg/L	19.1%	[66]
-COOH functionalized GO	Hg ²⁺	400 mg/L	12.2%	[67]
Chitosan/GO composite nanofibrous adsorbent	Cr ⁶⁺	10–1000 mg/L	31.04%	[71]

**Figure 3.** Van't Hoff fit curve (inset at the upper left corner: dependence of adsorption on temperature, at the lower right corner: values of adsorption thermodynamic functions). Reproduced under creative commons agreement from [64].

2.2. Silica Based Nanomaterials

Another important category of nanomaterials are Silica-based nanomaterials, which are widely used for removing HM ions owing to their non-toxicity and excellent surface characteristics [72,73]. The different possible interactions between mesoporous silica and metallic ions are shown in Figure 4. The surface of the mesoporous silica can also be functionalized with groups, such as amine ($-NH_2$) and thiol ($-SH$), which enhance interactions with heavy metal ions and their possible extraction from water. Table 4 summarizes previous studies reporting the functionalization of mesoporous silica applied to heavy metal ion removal.

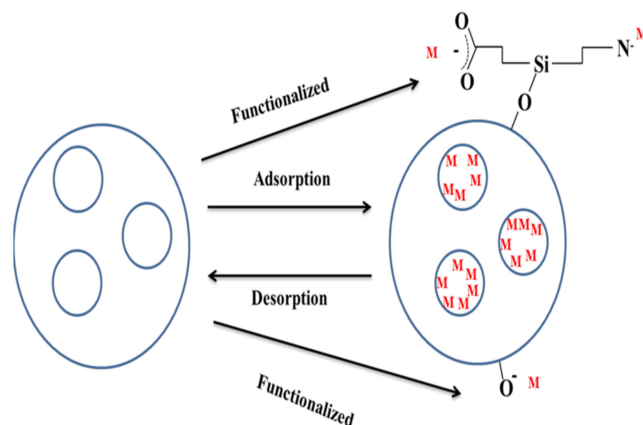


Figure 4. Adsorption sites of a mesoporous silica nanoparticles and functionalization with different groups.

The efficiency of amino-functionalized silica gel, silica hollow nanospheres, and amino-functionalized hollow silica nanospheres was investigated for the removal of Cd^{2+} , Ni^{2+} , and Pb^{2+} in batch mode. The adsorption capacity was found to decrease in the order of $\text{Pb}^{2+} > \text{Cd}^{2+} > \text{Ni}^{2+}$ for all of the adsorbents, which was attributed by the authors to the higher electronegativity of Pb^{2+} leading to stronger interactions with the negatively charged adsorbent surface. The maximum adsorption capacities (q_m) for uncoated silica hollow nanospheres as an adsorbent were found to be 8.375 mg/g (Ni^{2+}), 25.924 mg/g (Cd^{2+}), and 31.291 mg/g (Pb^{2+}). This adsorption increased to 26.858 mg/g, 54.351 mg/g, and 96.786 mg/g for amino-functionalized silica gel [74]. In another study, Nanopolyaniline and crosslinked nanopolyaniline based nanocomposites were studied for the removal of Cu^{2+} , Cd^{2+} , Hg^{2+} , and Pb^{2+} using a batch technique [72]. The adsorption capacity values for Pb^{2+} , Cu^{2+} , Hg^{2+} , and Cd^{2+} were found to be 341.4 mg/g, 289.8 mg/g, 162.9 mg/g, and 146.7 mg/g respectively. Selective Hg^{2+} removal by thiol-functionalized, porous, organic polymer-based nano-trap has an adsorption capacity of >1000 mg/g. Particularly, the material showed high stability in water under a wide pH range, which was attributed to its stable C–C bond; it also remained stable at high temperatures of up to 270 °C. The removal of 10 ppm of Cu^{2+} and cationic thiazine dyes using 3-aminopropyl and phenyl groups-based silica nanospheres was investigated in static mode. The absorption of Cu^{2+} ions reached 70% in 1 h, and thereafter increased to 80% after 2.5 h [75].

Table 4. Silica based materials for the adsorption of heavy metals.

Adsorbent	Target Metal	Initial Concentration	Removal%	References
Thiol and Amino functionalized SBA-15 Silica	Hg^{2+}	10.1 mg/L	29.2%	[76]
Amino functionalized mesoporous silica	Cr^{6+}	40 mg/L	8.205%	[77]
Functionalized silica with –SH	Hg^{2+}	-	50.5%	[78]
Amino functionalized silica gel in Tea Polyphenol extracts	Pb^{2+}	5–1200 mg/L (Pb^{2+}) 5–800 mg/L (Cu^{2+})	98.1%	[79]
Amino-functionalized and pure silica nano hollow sphere (NH_2 -SNHS, SHNS) and silica gel(NH_2 -SG)	Ni^{2+}	100 mg/L	0.84% (SHNS), 2.59% (NH_2 -SG), and 3.13% (NH_2 -SNHS) mg/g	[74]

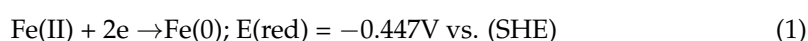
Table 4. Cont.

Adsorbent	Target Metal	Initial Concentration	Removal%	References
Amino-functionalized and pure silica nano hollow sphere (NH ₂ -SNHS, SHNS) and silica gel(NH ₂ -SG)	Pb ²⁺	100 mg/L	26.85%(SHNS), 54.35%(NH ₂ -SG), and 96.78%(NH ₂ -SNHS)	[74]
Amino functionalized silica gel in Tea Polyphenol extracts	Cd ²⁺	5–800 mg/L	99.78%	[74]
Organically functionalized silica gel	Cu ²⁺	63 mg/L	1.99%	[80]
Amino-functionalized and pure silica nano hollow sphere (NH ₂ -SNHS, SHNS) and silica gel(NH ₂ -SG)	Cd ²⁺	100 mg/L	2.6% (SHNS), 3.2% (NH ₂ -SG), and 4.1% (NH ₂ -SNHS)	[74]
Ionic liquid-functionalized silica	Pb ²⁺	50–200 mg/L	20.23% and	[81]
Amino functionalized silica gel in Tea Polyphenol extracts	Cu ²⁺	5–800 mg/L	99.59%	[79]
Ionic liquid-functionalized silica	Cd ²⁺	50–200 mg/L	15%	[76]

This highlights that heavy metal ions have different affinities for organic groups and their extraction can be tuned depending on the targeted metal ions. One shortcoming of the silica-based materials is the poor stability of the –Si–O–Si– bond in basic conditions, which may cause leaching of the surface-grafted functional groups.

2.3. Zero-Valent Iron Nanoparticles

Zero-valent metal nanoparticles have demonstrated their ability in remediating a variety of pollutants in wastewaters [82]. For instance, Ag NP are more particularly used for disinfecting wastewater owing to their antimicrobial/antifungal properties [83]. Nanoscale zero-valent iron (nZVI) can be defined as a composite consisting of Fe(0) and ferric oxide coating [84]. The nanosize of nZVI results in a higher surface to volume ratio or higher specific surface, which leads to an increased removal of pollutants [85]. Therefore, they have received considerable attention in the scientific community as a novel adsorbent to remediate a variety of heavy metals, including Hg²⁺, Cr⁶⁺, Cu²⁺, Ni²⁺, and Cd²⁺ [86–88]. In fact, nZVI is an excellent electron donor (see Equation (1)) with a reduction potential greater than -0.447 V, highly capable of reducing pollutants; the feasibility of the reduction depends on the redox potential of particular metal ions. For example, metal ions such as Zn or Cd have lower or almost similar reduction potential (i.e., -0.76 V and -0.40 V vs. Standard Hydrogen Electrode (SHE), respectively) than that of Fe, which interrupts the surface redox phenomenon of nZVI [89]. Subsequently, the removal of a particular pollutant (i.e., heavy metal ions) can occur through various processes such as precipitation, complexation, adsorption, oxidation, and reduction, which are briefly schematized in Figure 5.



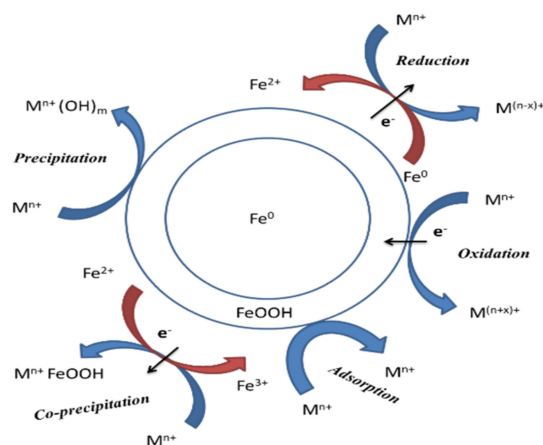


Figure 5. Schematic of a ZVI depicting several interaction mechanisms with heavy metals.

In spite of the noteworthy effectiveness of nZVI in the removal of heavy metal ions, its shortcomings cannot be neglected. For example, it was reported that nZVI oxidizes in air and in aqueous solutions, which results in the slowdown of the reduction processes of heavy metal ions [90]. Moreover, some scientific investigations have also suggested a tendency to agglomerate, which consequently decreases the reaction surface area and mobility [84]. Therefore, to improve its performance, several modification strategies, such as surface chemical modification or doping nZVI with other metals (Pd, Cu, Ni, and Pt) were investigated [91]. These modified nZVI showed an improvement in the removal of metallic pollutants. For example, in order to evaluate removal capacity of Cr^{6+} , Huang et al. studied a surface modified nZVI material formed by combining nZVI with sodium dodecyl sulfate (SDS). They measure an adsorption capacity of 253.68 mg/g with 300 mg/L initial Cr^{6+} concentration in batch adsorption experiments. This study demonstrated an improved adsorption capacity and a decreased aggregation of the modified nanomaterial [92]. In another study, nZVI and Au-doped nZVI nanoparticles were investigated for the removal of both Cd^{2+} and nitrates from water in batch mode [93]. They highlighted that increased pH and negative charge contributed to a significant increase in the Cd^{2+} removal capacity (from 40 mg/g to 188 mg/g) if nitrates are present in the water. The nZVI deposited with 1 wt.% Au reduced the nitrate quantity to less than 3% of the initial value, while maintaining a high Cd^{2+} removal capacity.

2.4. Magnetic Nanoparticles

Even though the nanomaterials described above showed an enormous capacity in the extraction of heavy metals, they carry certain limitations with regards to their cost-effectiveness, reusability, separation from aqueous solutions, and complex synthesis routes, which impede their utilization at a commercial scale. During the last two decades, micro and nano-scaled magnetic particles have attracted attention as adsorbents for eliminating the biological molecules, organic pollutants, and heavy metal ions from water and wastewater [94]. The major advantage with magnetic nanomaterials lies in their easy recovery after exhaustion from the treated solution by applying an external magnetic field, as shown in one of the studies carried out using magnetic mesoporous silica nanospheres for the extraction of Pb^{2+} , Hg^{2+} , and Pd^{2+} (Figure 6) [95].

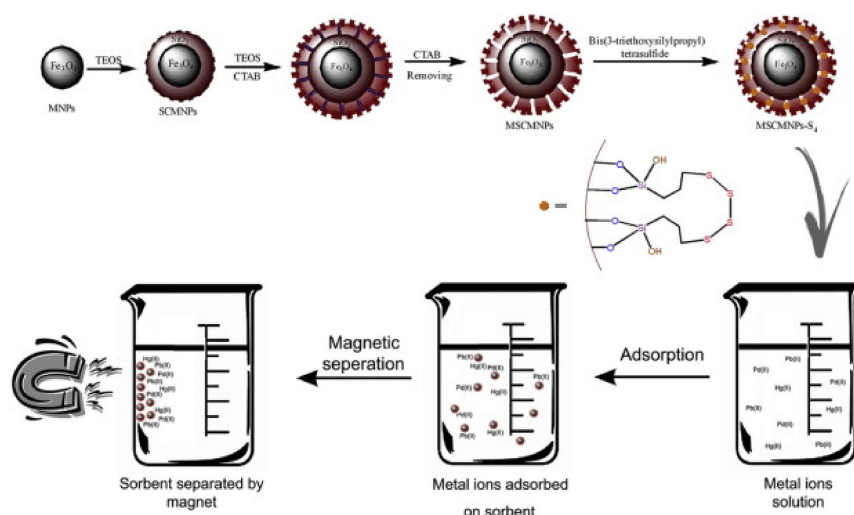


Figure 6. Schematic showing the mechanism of the magnetic nanoparticles in the removal of heavy metals. Reproduced with permission from [95].

2.4.1. Magnetic Iron-Oxide Nanoparticles

Among the magnetic materials, magnetic iron-oxide NP, i.e., magnetite (Fe_3O_4) and maghemite ($\gamma\text{-Fe}_2\text{O}_3$) present substantial dominance over conventionally used metal and alloy based magnetized nanomaterials in terms of facile synthesis, corrosion, and abrasion resistance. Maghemite and magnetite NP are extensively studied for wastewater treatment and heavy metal ion removal in particular [96]. Some studies investigating magnetic iron oxide NP for heavy metal ion removal are summarized in Table 5. Maghemite NP possess a large surface area, which contributes to their high adsorption capacity and are moreover environmental-friendly [97].

Akhbarizadeh et al. studied the removal of Cu^{2+} , Ni^{2+} , Mn^{2+} , Cd^{2+} , and Cr^{6+} using maghemite NP with initial concentration of 50 mg/L. They observed removal efficiencies of 88.2% for Cu, 84.4% for Cr, 18.3% for Mn, 15.7% for Ni, and 8.4% for Cd [98]. This study also indicated that removal of these five different metal ions by maghemite reached an equilibrium after a short period (10 min). Moreover, the absorption showed a good fit for Langmuir isotherm verifying the monolayer coverage of metallic ions on maghemite surface. In fact, authors highlighted a pH dependence during the extraction, when other effective parameters were kept constant (see Figure 7). The removal efficiency of copper increased from 8.4% to 50% when the pH was increased from 3 to 5. This study shows that selective removal of particular metal ions is feasible with these magnetic nanomaterials.

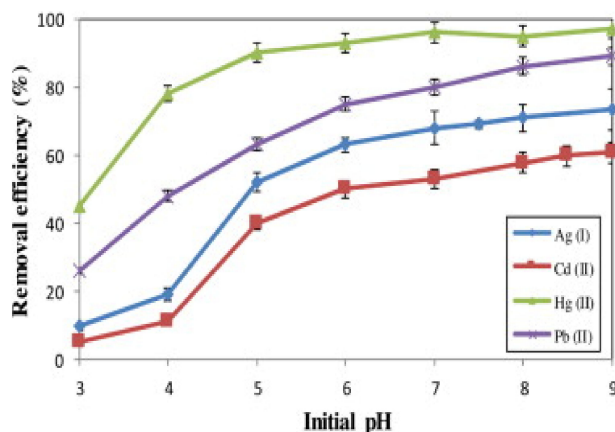


Figure 7. Removal efficiency with varying pH (polymer encapsulated maghemite). Reproduced with permission from [98].

In recent years, several reports on polymer-modified maghemite nanomaterials have been published. For example, Madrakian et al. prepared a novel mercaptoethylamino monomer-modified maghemite nanomaterial (MAMNPs) [99]. The maximum removal capacities of Ag^+ , Hg^{2+} , Pb^{2+} , and Cd^{2+} were 260.55 mg/g, 237.60 mg/g, 118.51 mg/g, and 91.55 mg/g respectively and the adsorption fitted the Sips isotherm model, which is the combination of Langmuir and Freundlich models. The Sips isotherm model is used for predicting the adsorption in heterogeneous systems and circumventing the limitation of the rising adsorbate concentration associated with the Freundlich isotherm [100]. The removal efficiency for cadmium increased from 8.7% to 50% when the pH was increased from 3 to 5 (Figure 7). This illustrates the efficiency of polymer-coated maghemite NP over pure maghemite NP. These modified maghemite NP showed good removal capabilities and selectivity towards various heavy metal ions. The removal of Cu^{2+} and other metallic ions using mesoporous magnetite NP was also investigated and the study showed a removal efficiency of 90% for a solution containing 50 mg/L of Cu^{2+} ions [101]. However, the adsorption followed the pseudo-second-order kinetic model deciphering a chemisorptive adsorption of metal ions on the magnetite NP. The experimental data followed the Langmuir isotherm, indicating the monolayer adsorption mechanism. Interestingly, the magnetic NP could be used for five consecutive cycles, demonstrating their high removal capacity. Shipley et al. studied the removal of Cu^{2+} using hematite NP and obtained a removal efficiency of 89% for an initial metal concentration ranging from 0.016 mg/L [102], which is lower in comparison with magnetic NP used by Fato et al., for Cu^{2+} removal. These results conclude the effectiveness and efficiency of magnetic NP over other adsorbents.

Superparamagnetic iron oxide NP (Fe_3O_4) were investigated for the treatment of synthetic water contaminated with Mn^{2+} , Zn^{2+} , Cu^{2+} , and Pb^{2+} ions [103]. In their study, the authors estimated an adsorption capacity of 11.5 mg/g, 12.4 mg/g, 14.5 mg/g, and 16.4 mg/g for Mn^{2+} , Zn^{2+} , Cu^{2+} , and Pb^{2+} ions respectively. The superparamagnetic ascorbic acid-coated Fe_3O_4 NP were synthesized and studied for their potential to remove arsenic ions from wastewater [104]. They found a maximum adsorption capacity of 46.06 mg/g and 16.56 mg/g for As^{3+} and As^{5+} respectively, as followed by Langmuir isotherm. In another study, Fe_2O_3 NP encapsulated in cellulose matrix were investigated for the removal of arsenic from aqueous solution [105]. The experimental results showed an excellent adsorption capacity towards As^{3+} and As^{5+} (23.16 mg/g and 32.11 mg/g, respectively) and the experimental data followed both Langmuir and Freundlich isotherms. These studies show that cellulose encapsulated Fe_2O_3 NP exhibit a higher As^{5+} adsorption capacity with multilayered adsorption compared to superparamagnetic ascorbic acid-coated Fe_3O_4 NP. This increased adsorption might be due to the stronger interactions of As^{5+} with OH groups by forming a sodium arsenate complex. However, in environmental conditions arsenic is present in the form of hydrides. The higher adsorption for As^{3+} with ascorbic acid coated magnetic NP is probably due to its higher affinity to form methyl arsenic acid. Through these studies, we can conclude that polymer coated Fe_3O_4 NP can increase the adsorption affinity for some specific metallic ions and can be used for selective removal of heavy metals.

Table 5. Iron-oxide magnetic NP utilized for the removal of metallic ions from contaminated water.

Adsorbent	Target Metal/s	Initial Concentration	Removal%	References
Hematite-Magnetite hybrid	Pb^{2+}	2 mg/L	97.67%,	[106]
Hematite-Magnetite hybrid	Cd^{2+}	2 mg/L	99.84%	[106]
Maghemite NP	As^{5+}	1–11 mg/L	50%	[97]
Hematite-Magnetite hybrid	Cr^{3+}	2 mg/L	99.50%	[106]
Maghemite NP	Cr^{6+}	5–200 mg/L	1.92%	[107]
Biogenic nano-magnetite	Cr^{6+}	16.69 mg/L	3.2%	[108]
Magnetite NP	Pb^{2+}	10–600 mg/L	3730%	[103]

Table 5. Cont.

Adsorbent	Target Metal/s	Initial Concentration	Removal%	References
Magnetite NP	Mn ²⁺	10–600 mg/L	7700%	[103]
Carboxyl functionalized magnetite NP	Cu ²⁺	10 mg/L	0.983%	[109]
Carboxyl functionalized magnetite NP	Cd ²⁺	10 mg/L	1.03%	[109]
Magnetite NP	Zn ²⁺	10–600 mg/L	1046%	[103]

CuFe₂O₄ magnetic nanoparticles were prepared from industrial sludge and used as an adsorbent for the removal of Cd²⁺ ions. Experimental results show that at very low pH ~ 2.0, they observed negligible adsorption, whereas almost 99.9% adsorption occurred at pH 6.0 [110]. They observed fast removal of cadmium ions during the initial 10 min and thereafter a decrease in removal was observed until equilibrium was attained 20 min later. The Cd²⁺-CuFe₂O₄ interaction was described by the pseudo-second-order mechanism. The adsorption process followed the Langmuir adsorption isotherm with the monolayer adsorption capacity 13.87 mg/g at 298 K, which increased slightly to 17.54 mg/g at 318 K, indicating endothermic interactions. The removal of Ni²⁺ was investigated using Fe₃O₄ magnetic nanoparticle impregnated tea waste [111]. The removal efficiency decreased from 99 to 87% with the increase of initial concentration of Ni²⁺ in solution from 50 to 100 mg/L. In addition, the adsorption of Ni²⁺ increased with the increasing temperature from 303 to 323 K, which again highlights the endothermic nature of the adsorption process. However, in this study, the experimental data fit with both Langmuir and Freundlich models revealing a maximum adsorption capacity of 38.3 mg/g.

The efficient mixing of nanoparticles in contaminated water is seen as one of the major challenges for magnetic extraction of pollutants. It seems complicated to use magnetic nanomaterials for heavy metals removal at industrial scales. In fact, the efficient mixing of magnetic nanoparticles in solution requires appropriate micromixers. With that aim, Karvelas et al. investigated a Y-shaped micromixer to remove heavy metals from the contaminated water [112]. They observed that a higher mixing in the micromixer leads to slower adsorption, whereas the adsorption capacity increases with lower mixing of the NP with heavy metals. In their study, the faster adsorption leads to lower adsorption capacity.

2.4.2. Magnetic Nanocomposites

Magnetic nanocomposites are receiving an increased attention because of their easy recovery after exhaustion from water with the help of a magnet [113]. In general, magnetic nanocomposites are mostly based on magnetic iron oxide nanomaterials. In fact, the fabrication of these magnetic nanocomposites can be achieved through three approaches: (1) modifying the NP surface with functional groups such as –NH₂ and –SH; (2) coating the iron/iron oxide nanoparticles with other materials, such as humic acid, polyethylenimine, polyrhodanine, MnO₂ and polypyrrole, in order to make a core-shell structure; and (3) decorating porous materials such as graphene oxide and CNT with iron/iron oxide nanoparticles [114,115].

Polymer-functionalized Fe₂O₃ nanomaterials have been investigated for the removal of divalent Cu, Ni, and Co metal NP over a pH range of 3.5 to 10 [116]. The experimental results showed the highest removal efficiency for Cu(II) with the adsorption capacity of 6.98 mg/g at pH of 5.3. Ferric and ferrous chlorides are usually used for the synthesis of magnetite/zeolite nanocomposites. The synthesized nanocomposite possessed the composite ratio of 3:1 (zeolite: iron oxide) with saturation magnetization of 19.03 emu/g [117].

These NC were tested for the removal of Cs⁺ and Sr²⁺. They provided a maximum adsorption capacity of 207.4 mg/g and 83.68 mg/g for Cs⁺ and Sr²⁺ respectively. Fe@MgO nanocomposites were investigated for the removal of Pb²⁺ ions and methyl orange from contaminated water. These nanocomposites are a combination of strong magnetic nZVI nanoparticles and MgO, which exhibit a good adsorption capacity of 1476.4 mg/g and

6947.9 mg/g for Pb^{2+} ions and methyl orange respectively [118]. The experimental data followed the Langmuir linear regression model representing monolayer chemisorption of Pb^{2+} ions, as shown in Figure 8. Similarly, Guo et al. studied Pb^{2+} ion removal using rGO- Fe_3O_4 composite and reported an adsorption capacity of 373.14 mg/g [64], which is lower compared to other cited works. The different examples of magnetic nanocomposite-based adsorption studies are summarized in Table 6. The efficiency of superparamagnetic Iron Oxide Nanoparticles (SPIONs) and Chitosan-Coated SPIONs was tested for the removal of hexavalent chromium ions (with initial concentration of 1 mg/L) [119]. The experimental results showed a removal of 80.44% and 99.7% of Cr^{6+} ions for uncoated and Chitosan-coated SPIONs, respectively.

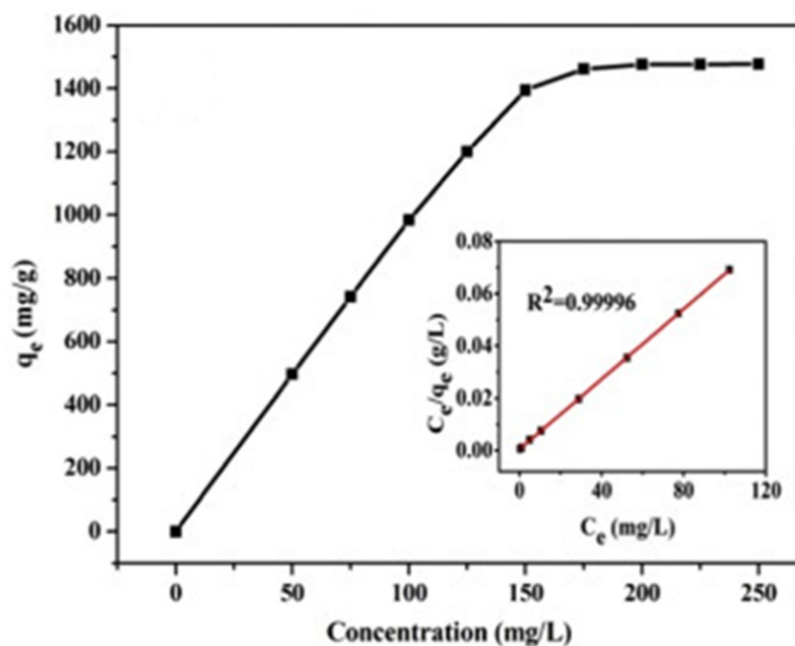


Figure 8. Langmuir fit for lead removal using Fe@MgO nanocomposites. Reproduced with permission from [118].

However, the complexity of using magnetic nanoparticles for water purification makes them complicated to apply at a larger scale and the overall cost-benefit ratio of magnetic nanoparticles is very high, which is a significant barrier for utilization at industrial scale. For this reason, research combining nanoparticles with membranes has spurred attention at it is seen as a more promising solution for larger scale water remediation [120]. For example, hydrogels have a 3D network structure that is capable of retaining water in their nanoporous structure. During the recent years, various composite membrane based nanoadsorbents were studied for the removal of heavy metals. Zhang et al. reported the removal of Cs ions using Clay–Hexacyanoferrate composite hydrogels [121]. The experimental results showed an adsorption capacity of 173 mg/g, even in 0.2 mg/L Cs contaminated water. Many nanocomposites have been studied for the adsorption of $^{137}\text{Cs}^+$ at larger scales [122]. Various other hydrogel such as polyacrylic acid hydrogel, 2-acrylamido-2-methyl-1-propane sulfonic acid-based magnetic responsive hydrogels, magnetic-vinyl pyridine-based hydrogel are investigated for the removal of other metallic ions like Cu^{2+} , Ni^{2+} , Cd^{2+} , Co^{2+} , U^{6+} etc. [123]. These hydrogels can be recycled and reused, but the scientific findings reported a decrease in the removal efficiency. Therefore, an in-depth research is required on these hydrogel-based nanoadsorbents that can sustain their removal capacities.

Table 6. Summary of the removal studies on heavy metals using magnetic nanocomposites.

Adsorbent	Target Metal	Initial Concentration or Concentration Range	Removal Efficiency (%)	References
Silica coated magnetic nanocomposites	Pb ²⁺	5–120 mg/L	1.49%	[124]
Silica based hybrid organic inorganic magnetic nanocomposites(MNPs@SiO ₂ -TSD-TEOS)	Pb ²⁺	100 mg/L	41.7%	[125]
Silica based hybrid organic inorganic magnetic nanocomposites(MNPs@SiO ₂ -TSD-TEOS)	Ni ²⁺	100 mg/L	35.7%	[125]
o-Vanillin functionalized mesoporous silica-coated magnetite nanoparticles (Fe ₃ O ₄ @MCM-41)	Pb ²⁺	120 mg/L	15.57%	[126]
Silica coated iron oxide magnetic nanocomposites(Fe ₃ O ₄ @SiO ₂)	Pb ²⁺	10 mg/L	97%	[127]
Silica coated iron oxide magnetic nanocomposites(Fe ₃ O ₄ @SiO ₂)	Hg ²⁺	10 mg/L	94.12%	[127]
Polythiophene modified chitosan/magnetite nanocomposites	Hg ²⁺	0.02–100 mg/L	5.28%	[128]
Bismuthiol-II-immobilized magnetic nanoparticles	Cr ³⁺	-	>90%	[129]
Bismuthiol-II-immobilized magnetic nanoparticles	Cu ²⁺	-	>90%	[129]
Thiol-lignocellulose sodium bentonite (TLNB) nanocomposites	Cd ²⁺	(0.20–1.70) × 10 ³ mg/L	45.832%	[130]
Thiol-lignocellulose sodium bentonite (TLNB) nanocomposites	Zn ²⁺	(0.20–1.70) × 10 ³ mg/L	35.729%	[130]
Magnetic Chitosan Nanocomposites	Cd ²⁺	10 mg/L	92.1%	[131]
Water-soluble magnetic graphene nanocomposites	Cd ²⁺	NA	>85%	[114]
Functionalized magnetic Fe ₃ O ₄	Cu ²⁺	10 mg/L	96%	[132]
Functionalized magnetic Fe ₃ O ₄	Hg ²⁺	10 mg/L	96%	[132]
Fe@MgO nanocomposite	Pb ²⁺	100 mg/L	147.64%	[118]
Magnetic MWCNT	Cr ⁶⁺	1–25 mg/L	1.14%	[133]

2.4.3. Reusability of Magnetic Nanoparticles

Various studies have demonstrated that magnetic NP can be applied to the removal of metallic ions from contaminated water. However, for a cost-effective adsorbent, it is essential to study their reusability or recyclability. For example, Rivera et al. studied Cr⁶⁺ ion removal using 2 g/L of the magnetic magnetite NP. They measured an adsorption

capacity of up to 12.4 mg/g. The regeneration cycles of the magnetic nanomaterials showed a slight decrease (about 4%) in the removal efficiency, concluding that the nanomaterial can be reused for up to 4 cycles continuously [134]. Tao et al., showed an effective removal of heavy metal ions (Hg^{2+} and Pb^{2+}) using thiol-functionalized magnetic mesoporous microspheres [135]. After water treatment, the NP were separated from the water using a magnet and washed with a suitable eluent. The recycled NP were tested against similar heavy metals and were able to remove the metal ions with a similar efficiency. Recyclability tests were also conducted by Chen et al. on functionalized magnetic Fe_3O_4 nanoparticles. In order to study the possibility of reusing Fe_3O_4 NP, they were subjected to several loading and elution operations. The elution operations were carried out by shaking Fe_3O_4 NP, which contained maximum amounts of metal ions in 100.00 mL of 0.50 M HCl. Interestingly, they showed no significant decrease in the removal efficiencies even after seven adsorption-desorption cycles, with a decrease from 100% to 93% [132]. Fato et al. investigated the reusability of MNP using nitric acid as eluent and reported that even after five successive cycles, the MNP can be reused with no significant decrease in the removal efficiency [101]. In addition, these magnetic NP can be easily separated from the treated water, which turned out to be their major advantage over other technologies. However, the behavior of engineered nanoparticles and their regeneration and desorption capacities in real conditions need to be evaluated before commercialization.

3. Nanomaterial Modified Bioelectrochemical Systems for Enhanced Power Production and the Remediation of Heavy Metals

During the past few years, a technique based on the integration of electrochemical and biological processes, usually referred to as bioelectrochemical systems (BESs), has emerged for wastewater treatment. A typical BES setup consists of anodic and cathodic chambers separated by an ion-selective membrane with microorganisms as catalysts for the redox reactions. The organic matter is oxidized in the anode chamber owing to microbial metabolic activity responsible for producing electrons. These electrons then circulate through an external circuit towards the cathode where the reduction of target species i.e., nitrates, H^+ , CO_2 or HM ions occurs [136,137]. In particular, BES can be operated in two different modes: microbial fuel cell (MFC) and microbial electrolysis cell (MEC), depending upon the targeted process. The electrons produced on substrate oxidation at the anode, accelerate the reduction of targeted heavy metal ions [138]. Even though BES poses a great advantage in scavenging metallic ions, their performance is highly dependent on the electrode material, redox potential, and substrate oxidation. These influence the reduction efficiency of HM at the cathode and the output power of BES. During the past few years, various electrode materials have been investigated for enhancing the overall performance, especially for the reduction of HM in BES. Due to their unique properties, nanomaterials have attracted significant attention in the scientific world. Therefore, researchers are investigating nanostructured bioelectrochemical systems (BESs) that utilize microorganisms along with nanomaterials to mediate, facilitate, or catalyze the redox reactions at one or both the electrodes, which in turn enhances the power output of the BES.

3.1. Electrode Materials for Anode in BESs

3.1.1. Conventional Anode Materials

Generally, carbon based materials, i.e., graphite plates [139], graphite rods [140], graphite felt [141], carbon brush [142], and carbon paper [143], are widely used as anode materials due to their good conductivity, biofilm formation, and non-corrosive behavior [144]. For example, carbon brush was used as an anode in the MFC and their performance was evaluated under different temperature conditions ranging from 300–750. The maximum power output increased from 1160 mW/m^2 to 1561 mW/m^2 with variation in temperature [142]. An enhancement in the electrical output was observed when plasma-modified carbon paper was used as an anode in an air-cathode cylindrical shaped MFC setup [143]. The maximum power output obtained was 107 mW/m^2 . However, these

materials exhibit some limitations, such as lack of durability and higher cost. Carbon felt with 95.5% of carbon content is considered as a good candidate for anode but simultaneously offers a large resistance. Graphite rods manifest certain advantages in terms of good electrical conductivity, chemical stability, and lower costs for MFC applications. However, the availability of large surface areas for biofilm growth and redox reactions is a major drawback for them. Hence, anodes with graphite fiber brush were designed that showed enhanced MFC power production [145]. However, several metal-based materials have also been investigated for MFC anodes with advantages in terms of conductivity, robustness, and cost-effectiveness. It has also been reported that the doping of graphite anodes with Mn^{4+} , Fe_3O_4 , and Ni^{2+} increases power generation of MFCs [146]. Generally, MFCs generate lower output voltage in comparison with the overall cell potential because of several energy losses, i.e., activation, bacterial metabolism, mass transfer, and ohmic, which effect the performance of an MFC. In this regard, strategies, such as introducing mediators and increasing electrode surface area are employed in order to overcome these losses. However, one of the strategies includes the invasion of nanomaterials. Nevertheless, there are some reports on nanomaterial-based anodes that have demonstrated an increment in the power output of the MFCs.

3.1.2. Nanomaterial Modified Anode Materials

The anode in MFC can be upgraded by using nanomaterial coatings, which provide a high specific surface, an improved electron transfer and promote electroactive biofilm. These enhance the power output of the MFC, as shown in Figure 9 [147]. Iron oxide can facilitate the extracellular electron transfer through two pathways; within the biofilm in the form of an electrical conduit or at the interface by accumulation on the cell surface [148]. Most of the metal oxides are not conductive but nevertheless promote and enhance biofilm formation. Thus, in this regard, carbon conductive materials or fillers e.g., CNT, Graphene, etc., can enhance the electrical conductivity of the metal oxides and thereby increase the extracellular electron transfer from the organism to the anode. Zhao et al. studied the possible increase of bio-current generation using ionic liquid functionalized graphene nanosheets as an anode [149]. They showed that current density increases from 0.40 mA/m^2 to 2.8 mA/m^2 within 30 h if the carbon paper anode is replaced with graphene nanosheets. The continuous testing on bare pencil graphite electrode (PGE), $\alpha\text{-MnO}_2/\text{PGE}$, PANI/PGE, and $\alpha\text{-MnO}_2/\text{PANI}/\text{PGE}$ were evaluated in glucose-fed-*Escherichia coli*-based MFC.

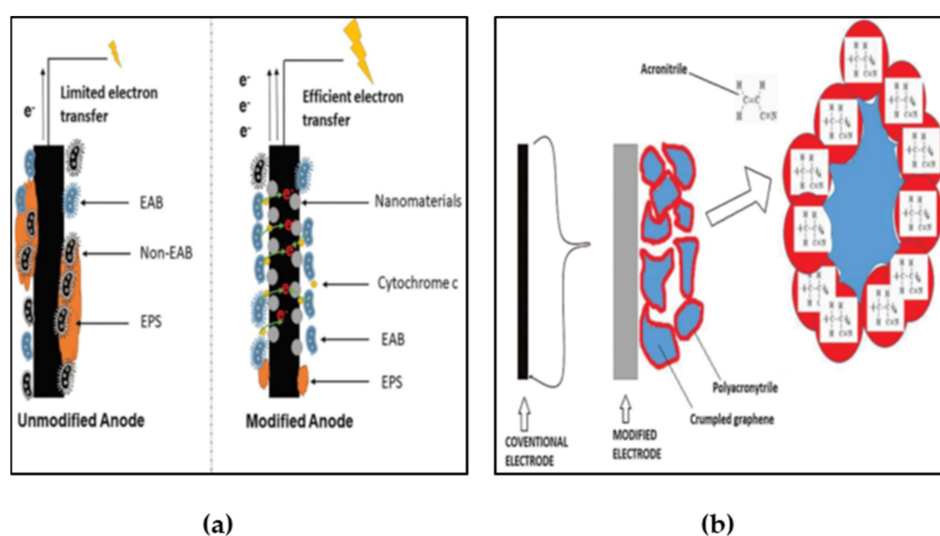


Figure 9. (a) General picture of nanomaterial modified anode and (b) graphene modified anode. Reproduced from [147] under creative commons attribution license.

The experimental results showed that the α -MnO₂/PANI/PGE-coated anode showed highest current and power density, which was 6 times higher than for uncoated PGE. Polyaniline networks grown on graphene nanoribbon-coated carbon paper as anode was reported to potentially increase the performance of MFC. When the carbon paper anode was coated with graphene nanoribbons the current density increased from 0.52 mA/m² to 1.8 mA/m² [150]. The current density is dependent on the type of material used, as shown in Figure 10. Reduced graphene was also coated with Polyaniline (PANI) in carbon cloth [151]. Biosynthesized α -MnO₂-based polyaniline binary composite were investigated as a biocatalyst in MFC [152].

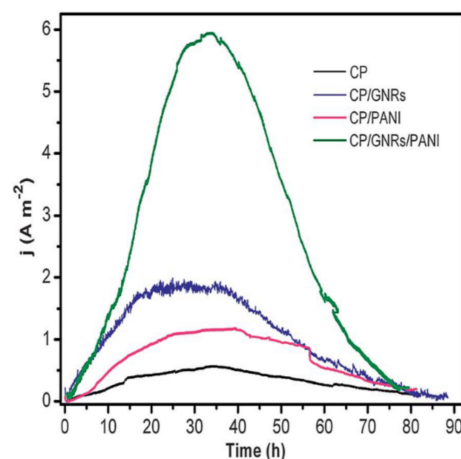


Figure 10. Current generation by *S. oneidensis* in ECs equipped with different anodes [150].

Similarly, the anode modified with reduced graphene oxide/tin oxide nanocomposite showed a significant increase of 4.8 times in the power density of MFC compared to its bare counterpart, as shown in the cyclic voltammetry curves reproduced with permission from [153] (see Figure 11a).

3.2. Electrode Materials for Cathode in BESs

3.2.1. Conventional Cathode Materials

Cathode performance is considered to be the main obstacle in the development of MFCs. Thus, the fabrication of cathode materials having high power generation and coulombic efficiency is the most crucial and challenging aspect for the development of successful MFC technology, more particularly for the treatment of metal-contaminated water. Graphite-based electrodes have been more extensively investigated for the removal of various heavy metal ions in water because of their low cost, high electrical conductivity, and biocompatibility. Several studies have reported findings that support electrochemical reduction of heavy metal ions at the biotic and abiotic cathode, summarized in Table 7 [154]. For instance, the removal of Cu²⁺ ions was studied via electrodeposition process at the cathode of MFC. A removal efficiency of >96% of Cu was estimated [155]. Moreover, the XRD analysis confirmed the reduction of Cu²⁺ to Cu⁺ and Cu⁰ on the electrode surface. The reduction was successfully achieved within 24 h of operation at the reduction potential of 0.347 V vs. Ag/AgCl. The reduced product was analyzed using ICP-MS, which indicated the deposition of elemental mercury over the cathode surface. Huang et al. studied the reduction of Cr (Cr^{6+/3+}) having initial concentration of 39.2 mg/L at the bio-cathode of MFC with a power production of 2.4 ± 0.1 W/m³ and at a current density of 6.9 A/m³ [156]. They concluded that initial Cr⁶⁺ concentration and solution conductivity have a clear effect on the biocathode MFC performance. In another study, carbon fiber cathode was used for the removal of chromium ions [157]. As a result, they observed 75.4% reduction of chromium ions with the maximum power density and current density of 970 mW/m² and 2462 mA/m². During the reduction process, the pH of the catholyte increased from 2 to

3.76, most likely due to the formation of $\text{Cr}(\text{OH})_3$ responsible for the basic environment. Based on the studies discussed, the bioelectrochemical remediation brings an alternative approach towards a cost-effective and ecofriendly degradation of heavy metals from the water. However, the reduction efficiency can be improved by introducing nanoadsorbents as the cathode.

Table 7. Carbon based materials as electrodes for bioelectrochemical reduction of heavy metals.

Target Metal	BES Configuration	Anode	Cathode	Power Output	Reference
Cr^{6+}	Double chambered MFC	Graphite plate	Graphite plate	150 mW/m^2	[158]
Hg^{2+}	Double chambered MFC	Graphite rod	Graphite rod	$32.6 \pm 0.5 \text{ W}/\text{m}^2$	[140]
Hg^{2+}	Double chambered MFC	Graphite felt	Carbon paper	433.1 mW/m^2	[159]
Cu^{2+}	Double chambered MFC	Carbon felt	Carbon plate	5.5 W/m^2	[160]
Ag^+	Double chambered MFC	Carbon brush	Carbon felt	4.25 mW/m^2	[161]
Se	Single chambered MFC	Carbon cloth	Carbon cloth	13–1500 mW/m^2 depending on initial concentration	[162]
Co	Double chambered MFC	Graphite felt	Graphite felt	258 mW/m^2	[163]
Ag^+	Double chambered MFC	Carbon felt	Carbon felt	0.109 mW/m^2	[164]

3.2.2. Nanomaterials Modified Cathode Materials

There are a very limited number of studies which have reported the use of nanomaterials as cathodes for the reduction of heavy metals. For the first time, Alumina-nickel nanoparticles-dispersed carbon nanofiber electrode were investigated for the removal of chromium ion in MFC. The experimental results showed a high reduction rate of $2.13 \text{ g}/\text{m}^3\text{-h}$ with achievable maximum power density and current density of $1540 \text{ mW}/\text{m}^2$ and $4560 \text{ mA}/\text{m}^2$ (see Figure 11) [165]. Shi et al. investigated graphite electrode modified with natural pyrrhotite for the reduction of Cr^{6+} in the MFC [166]. A removal of 99.59% was achieved within 10.5 h of operation with a maximum power density of $45.4 \text{ mW}/\text{m}^2$. However, the uncoated graphite cathode generated a maximum power density of $35.5 \text{ mW}/\text{m}^2$. This study demonstrated the efficiency of a naturally-occurring mineral in the effective removal of Cr ions. However, it also produced a lower output power and maximum removal was achieved at $\text{pH} = 3$, which suggest the use of additional chemicals to facilitate the reduction. Therefore, other cathode materials are explored to obtain a higher output power under ambient environmental conditions. Recently, graphene oxide-based catalysts were used at the cathode of MFC to enhance the recovery of Cu ions [167]. This study showed that Cu^{2+} could be efficiently removed in the rGO-MFC within 8 h of operation at the external resistance of 1000Ω . The removal efficiency reached 98% with the rGO-MFC for an initial Cu^{2+} concentration of 4, 8, and 12 mg/L and a maximum power output of $1.38 \text{ W}/\text{m}^2$. Nanocomposite-based electrocatalysts have also been investigated for the extraction of some heavy metals. For example, carbon cloth modified with $\alpha\text{-Fe}_2\text{O}_3$ /polyaniline nanocomposites were investigated for enhanced bioelectricity production and hexavalent chromium removal at the cathode of MFC [168]. The MFC showed a complete Cr^{6+} reduction at 50 mg/L with a reduction rate of $1.39 \text{ g}/\text{m}^3\text{-h}$ within 36 h of operation. However, they reported a maximum power density of $1502.78 \text{ mW}/\text{m}^2$, which was 1.753 times higher than carbon cloth cathode. Besides, $\alpha\text{-Fe}_2\text{O}_3$ /polyaniline modified electrode showed a reduction in the over-potential and favored electrocatalytic reduction of Cr with an increase in the current density as shown in the cyclic voltammetry curves with different electrode materials (Figure 11b). In another study, graphite felt modified with iron sulfide wrapped with reduced graphene oxide (FeS@rGO) nanocomposites are investigated for the removal of Cr^{6+} having initial concentration of 15 mg/L in MFC [169].

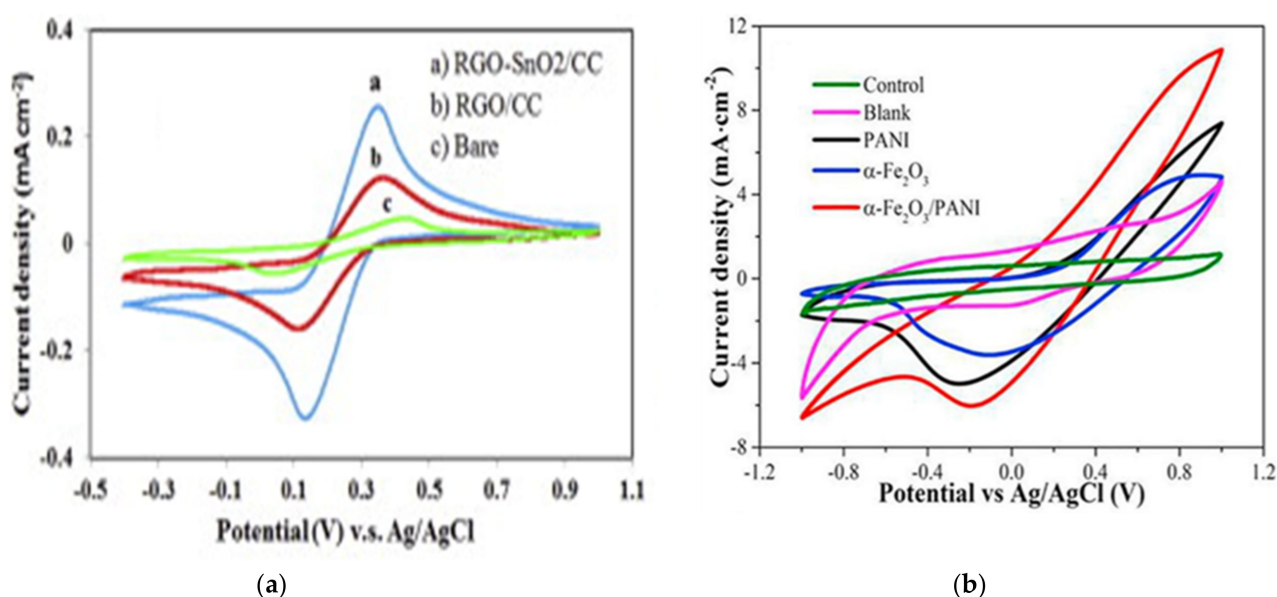


Figure 11. (a) Cyclic voltammograms of the bare CC, RGO/CC, and RGO-SnO₂/CC electrodes in 10 mM K₃[Fe(CN)₆] containing 0.1 M KCl (scan rate: 0.1 V/s). Reproduced with permission from [153] (b) Cyclic voltammetry curves with a potential range from −1.0 V to 1.0 V of various cathodes at the scanning rate of 1 mV/s in catholyte. Reproduced with permission from [165].

These nanocomposites showed 100% Cr⁶⁺ removal efficiency with the reduction rate of 1.43 mg/L/h. Overall, the improved electrochemical performance of MFC-FeS@rGO was expected due to the high conductivity, low internal resistance, and better reaction kinetics of FeS@rGO nanocomposites, as shown in Figure 12. A novel study representing the integrated setup of ZVI and MFC was investigated for the removal of As³⁺ with an initial concentration of 0.3 mg/L [170].

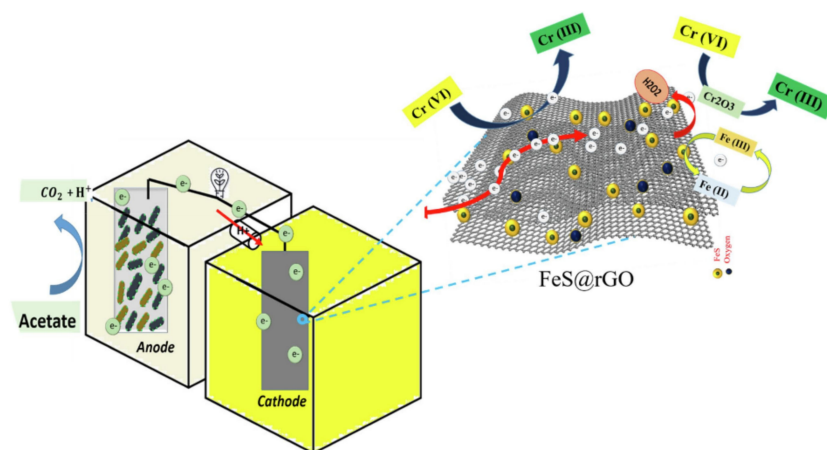


Figure 12. Possible mechanism of Cr(VI) reduction at FeS@rGO decorated cathode in MFC. Reproduced with permission from [169].

This study showed a more significant decrease in the concentrations of both the As³⁺ and total As using MFC-ZVI hybrid process than solely using ZVI. After 2 h of operation, the total As concentration remaining in the solution was only 9.8 µg/L and the As³⁺ concentration was below the detection limit in the case of the MFC-ZVI hybrid process. On the other hand, the residual total As concentration and As³⁺ concentration were 180 µg/L and 106 µg/L, respectively in the case of ZVI process. This corresponds to an improvement of 40% in the removal efficiency of total As. These results highlight a notable increase in the efficiency of As removal with the MFC-ZVI based hybrid. Such a combined technology

was studied only for the lower concentrations of artificially prepared As contaminated water. However, in real situations, the presence of other contaminants can interfere with the selective removal of As and in turn reduce the applicability of this technology for environmental samples.

4. Conclusions and Future Perspectives

4.1. Roadmap of the Nanomaterial Based Adsorbents for the Extraction of Heavy Metals

Due to the prevalent water crisis, nano-adsorbents are widely being investigated for the treatment of metal-contaminated waters owing to their exceptional properties, as described in this review. A variety of nanomaterials, including carbon-based nanotubes, graphene, silica-derived nanomaterials, ZVI, magnetic nanoparticles, and nanocomposites have been extensively discussed and critically analyzed. These nanomaterials exhibit a great potential as adsorbents for heavy metal ion removal from wastewater. However, there are still some notable shortcomings associated with these NM that need to be addressed in order to make them suitable for wastewater treatment at the industrial scale. For instance, the natural agglomeration of CNT results in a lower specific surface for adsorption, which reduces their adsorption capacities. Moreover, when it comes to their applicability at an industrial scale, their attachment to the filters should be strong enough to prevent their release in the treated water, as their toxicity remains debatable. Graphene-based nanomaterials face several limitations at the industrial scale. The large-scale production of GO nanoparticles requires a suitable reaction media. It is a chemically intensive process, which generates toxic by-products and can lead to serious environmental implications. CNT and graphene are also subject to clogging, similarly to activated carbon. These downsides of graphene-based adsorbents limit their large-scale implementation. Moreover, in the case of water treatment, it is difficult to separate them from the aqueous solution swiftly and efficiently due to their size. For this reason, the concept of nanocomposites seems to be a promising solution to solve the shortcomings of freestanding nanoscale adsorbents. Amongst these nanocomposites, magnetic nanocomposites possess some advantages in terms of their easy separation from treated waters using an external magnetic field, which shows potential in industrial applications.

4.2. Challenges and Opportunities for Large Scale Implementation of BESs for Heavy Metals Removal

Over the past few years, bioelectrochemical systems have emerged as a promising technology for heavy metal ion removal from contaminated water. However, their utilization at an industrial scale is still quite challenging due to their slow extraction rate and insufficient knowledge about the electron transfer mechanisms. The major challenge for implementing MFCs at larger scales is their inability to treat all type of metallic ions. The MFC setup can be used to reduce some of the heavy metals, i.e., Cu, Co, Hg, Cr, and Ag. It should be considered that only those metals which have a positive reduction potential can be spontaneously removed without any external applied voltage. For instance, Ni^{2+} has a reduction potential of -0.25 V and thus, cannot be reduced in MFC mode; therefore, it was investigated in MEC mode. The experimental results showed 33% and 9% removal efficiency of Ni^{2+} ions in MEC and MFC modes, respectively [171]. Interestingly, to overcome such issues, an innovative reactor configuration consisting of Cr-MFC and Cd-MFC in series was investigated for the removal of Cd ions with an achievable maximum output of 22.5 W/m^2 [172]. The MFCs in series enhance the power production and reduction of Cd ions. Another challenge that has been holding back the application of MFCs for the removal/recovery of heavy metals is the deterioration of performances and removal efficiencies based on the reactor configuration [173]. Both single-chambered MFC (SCMFC) and double-chambered MFC (DCMFC) are the most used designs for the removal of heavy metals. SCMFC has some notable advantages in terms of easy operation, cost effectiveness, and direct utilization of the substrate; but the lower coulombic efficiency contributes to the major drawback of this design [174,175]. In fact, the presence of membranes can maintain the ion balance and reduce the oxygen diffusion, which improves the coulombic

efficiency. However, the pH imbalance due to this membrane leads to potential losses and thus results in the deterioration of performances and removal efficiencies. Finally, besides the pH imbalance, the most important downside of MFCs is possible membrane fouling. This phenomenon occurs in the long-term operation of MFCs because of the unavoidable growth of biofilm on and outside the membrane which directly affects the overall power and current outputs of MFCs. Additionally, the separation membrane is expensive and contributes to about 38% of the total capital cost of MFCs [176], which is an obstacle, especially for scaling-up and future practical applications of MFCs. Owing to the interconnection between different components including anode, cathode, biofilm formation and power generation of MFC, the scaling-up of MFCs should not be limited to the augmentation of the anode volume. Additionally, appropriate amplification of electrodes, membranes and catalyst coatings should be analyzed.

4.3. Future Outlook for Nanomaterial Assisted BESs

Based on the studies reviewed, bioelectrochemical systems appear to be a promising technology for the removal of heavy metal ions. However, nanomaterial assisted bioelectrochemical-based hybrid technology shows an improved efficiency in terms of enhancing output power and accelerating the metal reduction reaction at the cathode. The nanomaterial-modified cathode manifested great potential for HM remediation, but the regeneration of the electrodes is a potential hindrance for the upscaling of this hybrid technology. Therefore, more extensive research on suitable recyclable electrode materials is required. Magnetic nanoadsorbents, owing to their facile recovery from treated water, are currently studied more particularly. They demonstrate potential for the selective removal of single component systems as well as multicomponent systems. However, despite promising pollutant removal capacities, the overall cost-benefit ratio of magnetic nanoparticles is very high, which is a significant barrier to utilization as main mean. To improve the cost effectiveness, it will be necessary to combine these magnetic nanoparticles with existing technologies. Based on the critical review on the various nanomaterials and nanomaterials based bioelectrochemical removal of HM, magnetic nanoparticles based cathodes can be further investigated for the treatment of metal-contaminated water. This can be achieved in two ways: (1) directly adding the MNP into the catholyte solution, which are easy to separate using an external magnetic field; and (2) coating the cathode with MNP, which may enhance the reduction efficiency on one hand but on the other hand, impede the recycling of MNP. However, this combined technology can be advantageous in terms of efficiency, cost-effectiveness, sustainability, and environmental friendliness. An additional advantage is the possibility to harvest energy during the removal process.

Author Contributions: R.K. has conceptualized and written the manuscript. E.R. and P.R. have extensively reviewed the manuscript and have contributed significantly to it. All authors have read and agreed to the published version of the manuscript.

Funding: This research has been supported by the European Regional Development Fund project grant number TK134 “Emerging orders in quantum and nanomaterials” EQUiTANT, EMÜ Astra project EMBio “Value-chain based bio-economy”, and Eesti Maaülikool (EMÜ) Bridge Funding grant number P200030TIBT.

Institutional Review Board Statement: Not applicable.

Informed Consent Statement: Not applicable.

Data Availability Statement: Not applicable.

Conflicts of Interest: The authors declare no conflict of interest.

References

1. Rogowska, J.; Cieszyńska-Semenowicz, M.; Ratajczyk, W.; Wolska, L. Micropollutants in treated wastewater. *Ambio* **2020**, *49*, 487–503. [[CrossRef](#)] [[PubMed](#)]

2. Ali, H.; Khan, E.; Ilahi, I. Environmental Chemistry and Ecotoxicology of Hazardous Heavy Metals: Environmental Persistence, Toxicity, and Bioaccumulation. *J. Chem.* **2019**, *2019*, 6730305. [[CrossRef](#)]
3. Gautam, P.K.; Gautam, R.; Banerjee, S.; Chattopadhyaya, M.; Pandey, J. Heavy metals in the environment: Fate, transport, toxicity and remediation technologies. In *Heavy Metals*; Nava Science Publishers: Plzen, Czech Republic, 2016; pp. 101–130.
4. Vardhan, K.H.; Kumar, P.S.; Panda, R.C. A review on heavy metal pollution, toxicity and remedial measures: Current trends and future perspectives. *J. Mol. Liq.* **2019**, *290*, 111197. [[CrossRef](#)]
5. Sharma, R.; Agrawal, M. Biological effects of heavy metals: An overview. *J. Environ. Biol. Acad. Environ. Biol. India* **2005**, *26*, 301–313.
6. Tchounwou, P.B.; Yedjou, C.G.; Patlolla, A.K.; Sutton, D.J. Heavy metal toxicity and the environment. *Exp. Suppl.* **2012**, *101*, 133–164. [[CrossRef](#)] [[PubMed](#)]
7. Dominguez-Benetton, X.; Varia, J.C.; Pozo, G.; Modin, O.; Ter Heijne, A.; Fransaer, J.; Rabaey, K. Metal recovery by microbial electro-metallurgy. *Prog. Mater. Sci.* **2018**, *94*, 435–461. [[CrossRef](#)]
8. Lesmana, S.O.; Febriana, N.; Soetaredjo, F.E.; Sunarso, J.; Ismadji, S. Studies on potential applications of biomass for the separation of heavy metals from water and wastewater. *Biochem. Eng. J.* **2009**, *44*, 19–41. [[CrossRef](#)]
9. Morais, S.; Costa, F.; Pereira, M. Heavy Metals and Human Health. *Environ. Health Emerg. Issues Pract.* **2012**, *10*, 227–245.
10. Tokar, E.J.; Benbrahim-Tallaa, L.; Waalkes, M.P. Metal ions in human cancer development. *Met. Ions Life Sci* **2011**, *8*, 375–401. [[PubMed](#)]
11. Jomova, K.; Valko, M. Advances in metal-induced oxidative stress and human disease. *Toxicology* **2011**, *283*, 65–87. [[CrossRef](#)]
12. Cruz-Olivares, J.; Martínez-Barrera, G.; Pérez-Alonso, C.; Barrera-Díaz, C.E.; Chaparro-Mercado, M.d.C.; Ureña-Núñez, F. Adsorption of Lead Ions from Aqueous Solutions Using Gamma Irradiated Minerals. *J. Chem.* **2016**, *2016*, 8782469. [[CrossRef](#)]
13. Khulbe, K.C.; Matsura, T. Removal of heavy metals and pollutants by membrane adsorption techniques. *Appl. Water Sci.* **2018**, *8*, 19. [[CrossRef](#)]
14. Lee, I.H.; Kuan, Y.-C.; Chern, J.-M. Equilibrium and kinetics of heavy metal ion exchange. *J. Chin. Inst. Chem. Eng.* **2007**, *38*, 71–84. [[CrossRef](#)]
15. Burakov, A.; Galunin, E.; Burakova, I.; Memetova, A.; Agarwal, S.; Tkachev, A.; Gupta, V. Adsorption of heavy metals on conventional and nanostructured materials for wastewater treatment purposes: A review. *Ecotoxicol. Environ. Saf.* **2017**, *148*, 702–712. [[CrossRef](#)] [[PubMed](#)]
16. Abdullah, N.; Yusof, N.; Lau, W.J.; Jaafar, J.; Ismail, A. Recent trends of heavy metal removal from water/wastewater by membrane technologies. *J. Ind. Eng. Chem.* **2019**, *76*. [[CrossRef](#)]
17. Kumar, V.; Shahi, S.; Singh, S. Bioremediation: An eco-sustainable approach for restoration of contaminated sites. In *Microbial Bioprospecting for Sustainable Development*; Springer: Berlin/Heidelberg, Germany, 2018; pp. 115–136.
18. Donati, E.R.; Sani, R.K.; Goh, K.M.; Chan, K.-G. Editorial: Recent Advances in Bioremediation/Biodegradation by Extreme Microorganisms. *Front. Microbiol.* **2019**, *10*. [[CrossRef](#)]
19. Hlihor, R.M.; Gavrilescu, M.; Tavares, T.; Favier, L.; Olivieri, G. Bioremediation: An Overview on Current Practices, Advances, and New Perspectives in Environmental Pollution Treatment. *Biomed. Res. Int.* **2017**, *2017*, 6327610. [[CrossRef](#)] [[PubMed](#)]
20. Jin, W.; Zhang, Y. Sustainable Electrochemical Extraction of Metal Resources from Waste Streams: From Removal to Recovery. *ACS Sustain. Chem. Eng.* **2020**, *8*, 4693–4707. [[CrossRef](#)]
21. Jin, W.; Hu, M.; Hu, J. Selective and Efficient Electrochemical Recovery of Dilute Copper and Tellurium from Acidic Chloride Solutions. *ACS Sustain. Chem. Eng.* **2018**, *6*, 13378–13384. [[CrossRef](#)]
22. Karbasi, M.; Alamdari, E.K.; Dehkordi, E.A. Electrochemical performance of PbCo composite anode during Zinc electrowinning. *Hydrometallurgy* **2019**, *183*, 51–59. [[CrossRef](#)]
23. Tahoon, M.A.; Siddeeg, S.M.; Salem Alsaiani, N.; Mnif, W.; Ben Rebah, F. Effective Heavy Metals Removal from Water Using Nanomaterials: A Review. *Processes* **2020**, *8*, 645. [[CrossRef](#)]
24. Babel, S.; Kurniawan, T.A. Low-cost adsorbents for heavy metals uptake from contaminated water: A review. *J. Hazard. Mater.* **2003**, *97*, 219–243. [[CrossRef](#)]
25. Yan, H.; Li, H.; Tao, X.; Li, K.; Yang, H.; Li, A.; Xiao, S.; Cheng, R. Rapid Removal and Separation of Iron(II) and Manganese(II) from Micropolluted Water Using Magnetic Graphene Oxide. *ACS Appl. Mater. Interfaces* **2014**, *6*, 9871–9880. [[CrossRef](#)] [[PubMed](#)]
26. Marsh, H.; Rodríguez-Reinoso, F. Chapter 8—Applicability of Activated Carbon. In *Activated Carbon*; Marsh, H., Rodríguez-Reinoso, F., Eds.; Elsevier Science Ltd.: Oxford, UK, 2006; pp. 383–453.
27. Saleem, J.; Shahid, U.B.; Hijab, M.; Mackey, H.; McKay, G. Production and applications of activated carbons as adsorbents from olive stones. *Biomass Convers. Biorefin.* **2019**, *9*, 775–802. [[CrossRef](#)]
28. Sarma, G.K.; Sen Gupta, S.; Bhattacharyya, K.G. Nanomaterials as versatile adsorbents for heavy metal ions in water: A review. *Environ. Sci. Pollut. Res.* **2019**, *26*, 6245–6278. [[CrossRef](#)] [[PubMed](#)]
29. Theron, J.; Walker, J.A.; Cloete, T.E. Nanotechnology and Water Treatment: Applications and Emerging Opportunities. *Crit. Rev. Microbiol.* **2008**, *34*, 43–69. [[CrossRef](#)] [[PubMed](#)]
30. Yaqoob, A.A.; Parveen, T.; Umar, K.; Mohamad Ibrahim, M.N. Role of Nanomaterials in the Treatment of Wastewater: A Review. *Water* **2020**, *12*, 495. [[CrossRef](#)]

31. Parvin, F.; Rikta, S.Y.; Tareq, S.M. 8—Application of nanomaterials for the removal of heavy metal from wastewater. In *Nanotechnology in Water and Wastewater Treatment*; Ahsan, A., Ismail, A.F., Eds.; Elsevier: Amsterdam, The Netherlands, 2019; pp. 137–157.
32. Yang, J.; Hou, B.; Wang, J.; Tian, B.; Bi, J.; Wang, N.; Li, X.; Huang, X. Nanomaterials for the Removal of Heavy Metals from Wastewater. *Nanomaterials* **2019**, *9*, 424. [\[CrossRef\]](#) [\[PubMed\]](#)
33. Lei, T.; Li, S.-J.; Jiang, F.; Ren, Z.-X.; Wang, L.-L.; Yang, X.-J.; Tang, L.-H.; Wang, S.-X. Adsorption of Cadmium Ions from an Aqueous Solution on a Highly Stable Dopamine-Modified Magnetic Nano-Adsorbent. *Nanoscale Res. Lett* **2019**, *14*, 352. [\[CrossRef\]](#) [\[PubMed\]](#)
34. Kumar, P.; Kumar, P. Removal of cadmium (Cd-II) from aqueous solution using gas industry-based adsorbent. *SN Appl. Sci.* **2019**, *1*, 365. [\[CrossRef\]](#)
35. Pyrzyńska, K.; Bystrzejewski, M. Comparative study of heavy metal ions sorption onto activated carbon, carbon nanotubes, and carbon-encapsulated magnetic nanoparticles. *Colloids Surf. A Physicochem. Eng. Asp.* **2010**, *362*, 102–109. [\[CrossRef\]](#)
36. El-sayed, M.E.A. Nanoadsorbents for water and wastewater remediation. *Sci. Total Environ.* **2020**, *739*, 139903. [\[CrossRef\]](#) [\[PubMed\]](#)
37. Smith, S.C.; Rodrigues, D.F. Carbon-based nanomaterials for removal of chemical and biological contaminants from water: A review of mechanisms and applications. *Carbon* **2015**, *91*, 122–143. [\[CrossRef\]](#)
38. Menezes, B.R.C.d.; Rodrigues, K.F.; Fonseca, B.C.d.S.; Ribas, R.G.; Montanheiro, T.L.d.A.; Thim, G.P. Recent advances in the use of carbon nanotubes as smart biomaterials. *J. Mater. Chem. B* **2019**, *7*, 1343–1360. [\[CrossRef\]](#) [\[PubMed\]](#)
39. Mujawar, M.; Sahu, J.; Abdullah, E.; Natesan, J. Removal of Heavy Metals from Wastewater Using Carbon Nanotubes. *Sep. Purif. Rev.* **2014**, *43*, 311–338. [\[CrossRef\]](#)
40. Bassyouni, M.; Mansi, A.E.; Elgabry, A.; Ibrahim, B.A.; Kassem, O.A.; Alhebeshy, R. Utilization of carbon nanotubes in removal of heavy metals from wastewater: A review of the CNTs' potential and current challenges. *Appl. Phys. A* **2019**, *126*, 38. [\[CrossRef\]](#)
41. Yu, G.; Lu, Y.; Guo, J.; Patel, M.; Bafana, A.; Wang, X.; Qiu, B.; Jeffries, C.; Wei, S.; Guo, Z.; et al. Carbon nanotubes, graphene, and their derivatives for heavy metal removal. *Adv. Compos. Hybrid. Mater.* **2018**, *1*, 56–78. [\[CrossRef\]](#)
42. Arora, B.; Attri, P. Carbon Nanotubes (CNTs): A Potential Nanomaterial for Water Purification. *J. Compos. Sci.* **2020**, *4*, 135. [\[CrossRef\]](#)
43. Zhang, X.; Cui, H.; Gui, Y.; Tang, J. Mechanism and Application of Carbon Nanotube Sensors in SF(6) Decomposed Production Detection: A Review. *Nanoscale Res. Lett* **2017**, *12*, 177. [\[CrossRef\]](#)
44. Alijani, H.; Shariatnia, Z. Synthesis of high growth rate SWCNTs and their magnetite cobalt sulfide nanohybrid as super-adsorbent for mercury removal. *Chem. Eng. Res. Des.* **2018**, *129*, 132–149. [\[CrossRef\]](#)
45. Gupta, A.; Vidyarthi, S.R.; Sankaramakrishnan, N. Enhanced sorption of mercury from compact fluorescent bulbs and contaminated water streams using functionalized multiwalled carbon nanotubes. *J. Hazard. Mater.* **2014**, *274*, 132–144. [\[CrossRef\]](#) [\[PubMed\]](#)
46. Gupta, S.; Bhatiya, D.; Murthy, C.N. Metal Removal Studies by Composite Membrane of Polysulfone and Functionalized Single-Walled Carbon Nanotubes. *Sep. Sci. Technol.* **2015**, *50*, 421–429. [\[CrossRef\]](#)
47. Robati, D. Pseudo-second-order kinetic equations for modeling adsorption systems for removal of lead ions using multi-walled carbon nanotube. *J. Nanostruct. Chem.* **2013**, *3*, 55. [\[CrossRef\]](#)
48. Farghali, A.A.; Abdel Tawab, H.A.; Abdel Moaty, S.A.; Khaled, R. Functionalization of acidified multi-walled carbon nanotubes for removal of heavy metals in aqueous solutions. *J. Nanostruct. Chem.* **2017**, *7*, 101–111. [\[CrossRef\]](#)
49. Elsehly, E.M.I.; Chechenin, N.G.; Bukunov, K.A.; Makunin, A.V.; Priselkova, A.B.; Vorobyeva, E.A.; Motaweh, H.A. Removal of iron and manganese from aqueous solutions using carbon nanotube filters. *Water Supply* **2015**, *16*, 347–353. [\[CrossRef\]](#)
50. Mallakpour, S.; Khadem, E. 8—Carbon nanotubes for heavy metals removal. In *Composite Nanoadsorbents*; Kyzas, G.Z., Mitropoulos, A.C., Eds.; Elsevier: Amsterdam, The Netherlands, 2019; pp. 181–210.
51. Faur-Brasquet, C.; Kadirvelu, K.; Le Cloirec, P. Removal of metal ions from aqueous solution by adsorption onto activated carbon cloths: Adsorption competition with organic matter. *Carbon* **2002**, *40*, 2387–2392. [\[CrossRef\]](#)
52. Hur, J.; Shin, J.; Yoo, J.; Seo, Y.-S. Competitive Adsorption of Metals onto Magnetic Graphene Oxide: Comparison with Other Carbonaceous Adsorbents. *Sci. World J.* **2015**, *2015*, 836287. [\[CrossRef\]](#) [\[PubMed\]](#)
53. Borji, H.; Ayoub, G.M.; Bilbeisi, R.; Nassar, N.; Malaeb, L. How Effective Are Nanomaterials for the Removal of Heavy Metals from Water and Wastewater? *Water Air Soil Pollut.* **2020**, *231*, 330. [\[CrossRef\]](#)
54. Rodríguez, C.; Briano, S.; Leiva, E. Increased Adsorption of Heavy Metal Ions in Multi-Walled Carbon Nanotubes with Improved Dispersion Stability. *Molecules* **2020**, *25*, 3106. [\[CrossRef\]](#)
55. Amin, M.T.; Alazba, A.A.; Manzoor, U. A Review of Removal of Pollutants from Water/Wastewater Using Different Types of Nanomaterials. *Adv. Mater. Sci. Eng.* **2014**, *2014*, 825910. [\[CrossRef\]](#)
56. Chowdhury, S.; Balasubramanian, R. Recent advances in the use of graphene-family nanoadsorbents for removal of toxic pollutants from wastewater. *Adv. Colloid Interface Sci.* **2014**, *204*, 35–56. [\[CrossRef\]](#) [\[PubMed\]](#)
57. Ali, I.; Basheer, A.A.; Mbianda, X.Y.; Burakov, A.; Galunin, E.; Burakova, I.; Mkrtchyan, E.; Tkachev, A.; Grachev, V. Graphene based adsorbents for remediation of noxious pollutants from wastewater. *Environ. Int.* **2019**, *127*, 160–180. [\[CrossRef\]](#)

58. Woo, Y.C.; Kim, S.-H.; Shon, H.K.; Tijing, L.D. Introduction: Membrane Desalination Today, Past, and Future. In *Current Trends and Future Developments on (Bio-) Membranes*; Basile, A., Curcio, E., Inamuddin, Eds.; Elsevier: Amsterdam, The Netherlands, 2019; pp. xxv–xlvii.
59. Smith, A.T.; LaChance, A.M.; Zeng, S.; Liu, B.; Sun, L. Synthesis, properties, and applications of graphene oxide/reduced graphene oxide and their nanocomposites. *Nano Mater. Sci.* **2019**, *1*, 31–47. [\[CrossRef\]](#)
60. Azizighannad, S.; Mitra, S. Stepwise Reduction of Graphene Oxide (GO) and Its Effects on Chemical and Colloidal Properties. *Sci. Rep.* **2018**, *8*, 10083. [\[CrossRef\]](#) [\[PubMed\]](#)
61. Xu, L.; Wang, J. The application of graphene-based materials for the removal of heavy metals and radionuclides from water and wastewater. *Crit. Rev. Environ. Sci. Technol.* **2017**, *47*, 1042–1105. [\[CrossRef\]](#)
62. Zhao, G.; Li, J.; Ren, X.; Chen, C.; Wang, X. Few-Layered Graphene Oxide Nanosheets As Superior Sorbents for Heavy Metal Ion Pollution Management. *Environ. Sci. Technol.* **2011**, *45*, 10454–10462. [\[CrossRef\]](#) [\[PubMed\]](#)
63. Wang, H.; Yuan, X.; Wu, Y.; Huang, H.; Zeng, G.; Liu, Y.; Wang, X.; Lin, N.; Qi, Y. Adsorption characteristics and behaviors of graphene oxide for Zn(II) removal from aqueous solution. *Appl. Surf. Sci.* **2013**, *279*, 432–440. [\[CrossRef\]](#)
64. Guo, T.; Bulin, C.; Li, B.; Zhao, Z.; Yu, H.; Sun, H.; Ge, X.; Xing, R.; Zhang, B. Efficient removal of aqueous Pb(II) using partially reduced graphene oxide-Fe₃O₄. *Adsorpt. Sci. Technol.* **2017**, *36*, 1031–1048. [\[CrossRef\]](#)
65. Tabish, T.A.; Memon, F.A.; Gomez, D.E.; Horsell, D.W.; Zhang, S. A facile synthesis of porous graphene for efficient water and wastewater treatment. *Sci. Rep.* **2018**, *8*, 1817. [\[CrossRef\]](#)
66. Zhang, C.-Z.; Chen, B.; Bai, Y.; Xie, J. A new functionalized reduced graphene oxide adsorbent for removing heavy metal ions in water via coordination and ion exchange. *Sep. Sci. Technol.* **2018**, *53*, 2896–2905. [\[CrossRef\]](#)
67. Awad, F.S.; Abouzied, K.M.; Abou El-Maaty, W.M.; El-Wakil, A.M.; Samy El-Shall, M. Effective removal of mercury(II) from aqueous solutions by chemically modified graphene oxide nanosheets. *Arab. J. Chem.* **2020**, *13*, 2659–2670. [\[CrossRef\]](#)
68. Zheng, S.; Hao, L.; Zhang, L.; Wang, K.; Zheng, W.; Wang, X.; Zhou, X.; Li, W.; Zhang, L. Tea Polyphenols Functionalized and Reduced Graphene Oxide-ZnO Composites for Selective Pb(2+) Removal and Enhanced Antibacterial Activity. *J. Biomed. Nanotechnol.* **2018**, *14*, 1263–1276. [\[CrossRef\]](#)
69. Arshad, F.; Selvaraj, M.; Zain, J.; Banat, F.; Haija, M.A. Polyethylenimine modified graphene oxide hydrogel composite as an efficient adsorbent for heavy metal ions. *Sep. Purif. Technol.* **2019**, *209*, 870–880. [\[CrossRef\]](#)
70. Chauke, V.P.; Maity, A.; Chetty, A. High-performance towards removal of toxic hexavalent chromium from aqueous solution using graphene oxide-alpha cyclodextrin-polypyrrole nanocomposites. *J. Mol. Liq.* **2015**, *211*, 71–77. [\[CrossRef\]](#)
71. Hadi Najafabadi, H.; Irani, M.; Roshanfekar, L.; Heydari Haratameh, A.; Haririan, I. Removal of Cu²⁺, Pb²⁺ and Cr⁶⁺ from aqueous solutions using a chitosan/graphene oxide composite nanofibrous adsorbent. *RSC Adv.* **2015**, *5*, 16532–16539. [\[CrossRef\]](#)
72. Mahmoud, M.E.; Fekry, N.A.; El-Latif, M.M.A. Nanocomposites of nanosilica-immobilized-nanopolyaniline and crosslinked nanopolyaniline for removal of heavy metals. *Chem. Eng. J.* **2016**, *304*, 679–691. [\[CrossRef\]](#)
73. Nguyen, T.T.; Ma, H.T.; Avti, P.; Bashir, M.J.K.; Ng, C.A.; Wong, L.Y.; Jun, H.K.; Ngo, Q.M.; Tran, N.Q. Adsorptive Removal of Iron Using SiO₂ Nanoparticles Extracted from Rice Husk Ash. *J. Anal. Methods Chem.* **2019**, *2019*, 6210240. [\[CrossRef\]](#)
74. Najafi, M.; Yousefi, Y.; Rafati, A.A. Synthesis, characterization and adsorption studies of several heavy metal ions on amino-functionalized silica nano hollow sphere and silica gel. *Sep. Purif. Technol.* **2012**, *85*, 193–205. [\[CrossRef\]](#)
75. Kotsyuda, S.S.; Tomina, V.V.; Zub, Y.L.; Furtat, I.M.; Lebed, A.P.; Vachlavikova, M.; Melnyk, I.V. Bifunctional silica nanospheres with 3-aminopropyl and phenyl groups. Synthesis approach and prospects of their applications. *Appl. Surf. Sci.* **2017**, *420*, 782–791. [\[CrossRef\]](#)
76. Liu, A.M.; Hidajat, K.; Kawi, S.; Zhao, D.Y. A new class of hybrid mesoporous materials with functionalized organic monolayers for selective adsorption of heavy metal ions. *Chem. Commun.* **2000**, 1145–1146. [\[CrossRef\]](#)
77. Li, X.; Han, C.; Zhu, W.; Ma, W.; Luo, Y.; Zhou, Y.; Yu, J.; Wei, K. Cr(VI) Removal from Aqueous by Adsorption on Amine-Functionalized Mesoporous Silica Prepared from Silica Fume. *J. Chem.* **2014**, *2014*, 765856. [\[CrossRef\]](#)
78. Li, R.; Zhang, L.; Wang, P. Rational design of nanomaterials for water treatment. *Nanoscale* **2015**, *7*, 17167–17194. [\[CrossRef\]](#)
79. Huang, X.; Wang, L.; Chen, J.; Jiang, C.; Wu, S.; Wang, H. Effective removal of heavy metals with amino-functionalized silica gel in tea polyphenol extracts. *J. Food Meas. Charact.* **2020**, *14*, 2134–2144. [\[CrossRef\]](#)
80. Wang, H.; Kang, J.; Liu, H.; Qu, J. Preparation of organically functionalized silica gel as adsorbent for copper ion adsorption. *J. Environ. Sci.* **2009**, *21*, 1473–1479. [\[CrossRef\]](#)
81. Wieszczycka, K.; Filipowiak, K.; Wojciechowska, I.; Buchwald, T.; Siwińska-Ciesielczyk, K.; Strzemieska, B.; Jesionowski, T.; Voelkel, A. Novel highly efficient ionic liquid-functionalized silica for toxic metals removal. *Sep. Purif. Technol.* **2021**, *265*, 118483. [\[CrossRef\]](#)
82. Crane, R.A.; Scott, T.B. Nanoscale zero-valent iron: Future prospects for an emerging water treatment technology. *J. Hazard. Mater.* **2012**, *211–212*, 112–125. [\[CrossRef\]](#) [\[PubMed\]](#)
83. Srinivasan, N.R.; Shankar, P.A.; Bandyopadhyaya, R. Plasma treated activated carbon impregnated with silver nanoparticles for improved antibacterial effect in water disinfection. *Carbon* **2013**, *57*, 1–10. [\[CrossRef\]](#)
84. O'Carroll, D.; Sleep, B.; Krol, M.; Boparai, H.; Kocur, C. Nanoscale zero valent iron and bimetallic particles for contaminated site remediation. *Adv. Water Resour.* **2013**, *51*, 104–122. [\[CrossRef\]](#)
85. Phenrat, T.; Lowry, G.V.; Babakhani, P. Nanoscale zerovalent iron (NZVI) for environmental decontamination: A brief history of 20 years of research and field-scale application. In *Nanoscale Zerovalent Iron Particles for Environmental Restoration: From Fundamental*

- Science to Field Scale Engineering Applications*; Phenrat, T., Lowry, G.V., Eds.; Springer International Publishing: Cham, Switzerland, 2019; pp. 1–43.
86. Liu, T.; Wang, Z.-L.; Sun, Y. Manipulating the morphology of nanoscale zero-valent iron on pumice for removal of heavy metals from wastewater. *Chem. Eng. J.* **2015**, *263*, 55–61. [\[CrossRef\]](#)
 87. Zhang, Z.; Hao, Z.W.; Liu, W.L.; Xu, X.H. Synchronous treatment of heavy metal ions and nitrate by zero-valent iron. *Huan Jing Ke Xue* **2009**, *30*, 775–779.
 88. Seyedi, S.M.; Rabiee, H.; Shahabadi, S.M.S.; Borghei, S.M. Synthesis of Zero-Valent Iron Nanoparticles Via Electrical Wire Explosion for Efficient Removal of Heavy Metals. *CLEAN Soil Air Water* **2017**, *45*, 1600139. [\[CrossRef\]](#)
 89. Guo, J.J.; Fan, M.D. Progress of Removing Heavy Metals by Zero Valent Iron Nanoparticles from Wastewater. *Adv. Mater. Res.* **2013**, *726–731*, 2563–2566. [\[CrossRef\]](#)
 90. Sarathy, V.; Tratnyek, P.G.; Nurmi, J.T.; Baer, D.R.; Amonette, J.E.; Chun, C.L.; Penn, R.L.; Reardon, E.J. Aging of Iron Nanoparticles in Aqueous Solution: Effects on Structure and Reactivity. *J. Phys. Chem. C* **2008**, *112*, 2286–2293. [\[CrossRef\]](#)
 91. Fu, F.; Dionysiou, D.D.; Liu, H. The use of zero-valent iron for groundwater remediation and wastewater treatment: A review. *J. Hazard. Mater.* **2014**, *267*, 194–205. [\[CrossRef\]](#)
 92. Huang, D.-L.; Chen, G.-M.; Zeng, G.-M.; Xu, P.; Yan, M.; Lai, C.; Zhang, C.; Li, N.-J.; Cheng, M.; He, X.-X.; et al. Synthesis and Application of Modified Zero-Valent Iron Nanoparticles for Removal of Hexavalent Chromium from Wastewater. *Water Air Soil Pollut.* **2015**, *226*, 375. [\[CrossRef\]](#)
 93. Su, Y.; Adeleye, A.S.; Huang, Y.; Sun, X.; Dai, C.; Zhou, X.; Zhang, Y.; Keller, A.A. Simultaneous removal of cadmium and nitrate in aqueous media by nanoscale zerovalent iron (nZVI) and Au doped nZVI particles. *Water Res.* **2014**, *63*, 102–111. [\[CrossRef\]](#)
 94. Tamjidi, S.; Esmaili, H.; Kamyab Moghadas, B. Application of magnetic adsorbents for removal of heavy metals from wastewater: A review study. *Mater. Res. Express* **2019**, *6*, 102004. [\[CrossRef\]](#)
 95. Vojoudi, H.; Badiei, A.; Bahar, S.; Mohammadi Ziarani, G.; Faridbod, F.; Ganjali, M.R. A new nano-sorbent for fast and efficient removal of heavy metals from aqueous solutions based on modification of magnetic mesoporous silica nanospheres. *J. Magn. Magn. Mater.* **2017**, *441*, 193–203. [\[CrossRef\]](#)
 96. Etale, A.; Tutu, H.; Drake, D.C. The effect of silica and maghemite nanoparticles on remediation of Cu(II)-, Mn(II)- and U(VI)-contaminated water by *Acutodesmus* sp. *J. Appl. Phycol.* **2016**, *28*, 251–260. [\[CrossRef\]](#)
 97. Tuutijärvi, T.; Lu, J.; Sillanpää, M.; Chen, G. As(V) adsorption on maghemite nanoparticles. *J. Hazard. Mater.* **2009**, *166*, 1415–1420. [\[CrossRef\]](#) [\[PubMed\]](#)
 98. Akhbarizadeh, R.; Shayestefar, M.R.; Darezereshki, E. Competitive Removal of Metals from Wastewater by Maghemite Nanoparticles: A Comparison Between Simulated Wastewater and AMD. *Mine Water Environ.* **2014**, *33*, 89–96. [\[CrossRef\]](#)
 99. Madrakian, T.; Afkhami, A.; Zadpour, B.; Ahmadi, M. New synthetic mercaptoethylamino homopolymer-modified maghemite nanoparticles for effective removal of some heavy metal ions from aqueous solution. *J. Ind. Eng. Chem.* **2015**, *21*, 1160–1166. [\[CrossRef\]](#)
 100. Tzabar, N.; ter Brake, H.J.M. Adsorption isotherms and Sips models of nitrogen, methane, ethane, and propane on commercial activated carbons and polyvinylidene chloride. *Adsorption* **2016**, *22*, 901–914. [\[CrossRef\]](#)
 101. Fato, F.P.; Li, D.-W.; Zhao, L.-J.; Qiu, K.; Long, Y.-T. Simultaneous Removal of Multiple Heavy Metal Ions from River Water Using Ultrafine Mesoporous Magnetite Nanoparticles. *ACS Omega* **2019**, *4*, 7543–7549. [\[CrossRef\]](#)
 102. Shipley, H.J.; Engates, K.E.; Grover, V.A. Removal of Pb(II), Cd(II), Cu(II), and Zn(II) by hematite nanoparticles: Effect of sorbent concentration, pH, temperature, and exhaustion. *Environ. Sci. Pollut. Res.* **2013**, *20*, 1727–1736. [\[CrossRef\]](#)
 103. Giraldo, L.; Erto, A.; Moreno-Piraján, J. Magnetite nanoparticles for removal of heavy metals from aqueous solutions: Synthesis and characterization. *Adsorption* **2013**, *19*. [\[CrossRef\]](#)
 104. Feng, L.; Cao, M.; Ma, X.; Zhu, Y.; Hu, C. Superparamagnetic high-surface-area Fe₃O₄ nanoparticles as adsorbents for arsenic removal. *J. Hazard. Mater.* **2012**, *217–218*, 439–446. [\[CrossRef\]](#)
 105. Yu, X.; Tong, S.; Ge, M.; Zuo, J.; Cao, C.; Song, W. One-step synthesis of magnetic composites of cellulose@iron oxide nanoparticles for arsenic removal. *J. Mater. Chem. A* **2013**, *1*, 959–965. [\[CrossRef\]](#)
 106. Ahmed, M.A.; Ali, S.M.; El-Dek, S.I.; Galal, A. Magnetite–hematite nanoparticles prepared by green methods for heavy metal ions removal from water. *Mater. Sci. Eng. B* **2013**, *178*, 744–751. [\[CrossRef\]](#)
 107. Hu, J.; Chen, G.; Lo, I.M. Removal and recovery of Cr(VI) from wastewater by maghemite nanoparticles. *Water Res.* **2005**, *39*, 4528–4536. [\[CrossRef\]](#) [\[PubMed\]](#)
 108. Watts, M.P.; Coker, V.S.; Parry, S.A.; Patrick, R.A.; Thomas, R.A.; Kalin, R.; Lloyd, J.R. Biogenic nano-magnetite and nano-zero valent iron treatment of alkaline Cr(VI) leachate and chromite ore processing residue. *Appl. Geochem.* **2015**, *54*, 27–42. [\[CrossRef\]](#)
 109. Shi, J.; Li, H.; Lu, H.; Zhao, X. Use of Carboxyl Functional Magnetite Nanoparticles as Potential Sorbents for the Removal of Heavy Metal Ions from Aqueous Solution. *J. Chem. Eng. Data* **2015**, *60*, 2035–2041. [\[CrossRef\]](#)
 110. Tu, Y.-J.; You, C.-F.; Chang, C.-K. Kinetics and thermodynamics of adsorption for Cd on green manufactured nano-particles. *J. Hazard. Mater.* **2012**, *235–236*, 116–122. [\[CrossRef\]](#) [\[PubMed\]](#)
 111. Panneerselvam, P.; Morad, N.; Tan, K.A. Magnetic nanoparticle (Fe₃O₄) impregnated onto tea waste for the removal of nickel(II) from aqueous solution. *J. Hazard. Mater.* **2011**, *186*, 160–168. [\[CrossRef\]](#) [\[PubMed\]](#)
 112. Karvelas, E.; Liosis, C.; Benos, L.; Karakasidis, T.; Sarris, I. Micromixing Efficiency of Particles in Heavy Metal Removal Processes under Various Inlet Conditions. *Water* **2019**, *11*, 1135. [\[CrossRef\]](#)

113. Mourdikoudis, S.; Kostopoulou, A.; LaGrow, A.P. Magnetic Nanoparticle Composites: Synergistic Effects and Applications. *Adv. Sci.* **2021**, *8*, 2004951. [[CrossRef](#)] [[PubMed](#)]
114. Zhang, W.; Shi, X.; Zhang, Y.; Gu, W.; Li, B.; Xian, Y. Synthesis of water-soluble magnetic graphene nanocomposites for recyclable removal of heavy metal ions. *J. Mater. Chem. A* **2013**, *1*, 1745–1753. [[CrossRef](#)]
115. Elmi, F.; Hosseini, T.; Taleshi, M.S.; Taleshi, F. Kinetic and thermodynamic investigation into the lead adsorption process from wastewater through magnetic nanocomposite Fe₃O₄/CNT. *Nanotechnol. Environ. Eng.* **2017**, *2*, 13. [[CrossRef](#)]
116. Takafuji, M.; Ide, S.; Ihara, H.; Xu, Z. Preparation of Poly(1-vinylimidazole)-Grafted Magnetic Nanoparticles and Their Application for Removal of Metal Ions. *Chem. Mater.* **2004**, *16*, 1977–1983. [[CrossRef](#)]
117. Faghihian, H.; Moayed, M.; Firooz, A.; Iravani, M. Evaluation of a new magnetic zeolite composite for removal of Cs⁺ and Sr²⁺ from aqueous solutions: Kinetic, equilibrium and thermodynamic studies. *C. R. Chim.* **2014**, *17*, 108–117. [[CrossRef](#)]
118. Ge, L.; Wang, W.; Peng, Z.; Tan, F.; Wang, X.; Chen, J.; Qiao, X. Facile fabrication of Fe@MgO magnetic nanocomposites for efficient removal of heavy metal ion and dye from water. *Powder Technol.* **2018**, *326*, 393–401. [[CrossRef](#)]
119. Samrot, A.V.; Sahithya, C.S.; Selvarani, A.J.; Pachiyappan, S.; Kumar, S.S. Surface-Engineered Super-Paramagnetic Iron Oxide Nanoparticles For Chromium Removal. *Int. J. Nanomed.* **2019**, *14*, 8105–8119. [[CrossRef](#)]
120. Rauwel, P.; Uhl, W.; Rauwel, E. Editorial for the Special Issue on ‘Application and Behavior of Nanomaterials in Water Treatment’. *Nanomaterials* **2019**, *9*, 880. [[CrossRef](#)] [[PubMed](#)]
121. Zhang, H.; Hodges, C.S.; Mishra, P.K.; Yoon, J.Y.; Hunter, T.N.; Lee, J.W.; Harbottle, D. Bio-Inspired Preparation of Clay–Hexacyanoferrate Composite Hydrogels as Super Adsorbents for Cs⁺. *ACS Appl. Mater. Interfaces* **2020**, *12*, 33173–33185. [[CrossRef](#)]
122. Rauwel, P.; Rauwel, E. Towards the Extraction of Radioactive Cesium-137 from Water via Graphene/CNT and Nanostructured Prussian Blue Hybrid Nanocomposites: A Review. *Nanomaterials* **2019**, *9*, 682. [[CrossRef](#)] [[PubMed](#)]
123. Perumal, S.; Atchudan, R.; Edison, T.N.J.I.; Babu, R.S.; Karpagavinayagam, P.; Vedhi, C. A Short Review on Recent Advances of Hydrogel-Based Adsorbents for Heavy Metal Ions. *Metals* **2021**, *11*, 864. [[CrossRef](#)]
124. Nicola, R.; Costişor, O.; Ciopec, M.; Negrea, A.; Lazău, R.; Ianăşi, C.; Picioruş, E.-M.; Len, A.; Almásy, L.; Szerb, E.I.; et al. Silica-Coated Magnetic Nanocomposites for Pb²⁺ Removal from Aqueous Solution. *Appl. Sci.* **2020**, *10*, 2726. [[CrossRef](#)]
125. Ahmad, N.; Sereshti, H.; Mousazadeh, M.; Rashidi Nodeh, H.; Kamboh, M.A.; Mohamad, S. New magnetic silica-based hybrid organic-inorganic nanocomposite for the removal of lead(II) and nickel(II) ions from aqueous solutions. *Mater. Chem. Phys.* **2019**, *226*, 73–81. [[CrossRef](#)]
126. Culita, D.C.; Simonescu, C.M.; Patescu, R.-E.; Dragne, M.; Stanica, N.; Oprea, O. o-Vanillin functionalized mesoporous silica—Coated magnetite nanoparticles for efficient removal of Pb(II) from water. *J. Solid State Chem.* **2016**, *238*, 311–320. [[CrossRef](#)]
127. Hu, H.; Wang, Z.; Pan, L. Synthesis of monodisperse Fe₃O₄@silica core-shell microspheres and their application for removal of heavy metal ions from water. *J. Alloy. Compd.* **2010**, *492*, 656–661. [[CrossRef](#)]
128. Morsi, R.E.; Al-Sabagh, A.M.; Moustafa, Y.M.; ElKholy, S.G.; Sayed, M.S. Polythiophene modified chitosan/magnetite nanocomposites for heavy metals and selective mercury removal. *Egypt. J. Pet.* **2018**, *27*, 1077–1085. [[CrossRef](#)]
129. Suleiman, J.S.; Hu, B.; Peng, H.; Huang, C. Separation/preconcentration of trace amounts of Cr, Cu and Pb in environmental samples by magnetic solid-phase extraction with Bismuthiol-II-immobilized magnetic nanoparticles and their determination by ICP-OES. *Talanta* **2009**, *77*, 1579–1583. [[CrossRef](#)]
130. Zhang, W.; An, Y.; Li, S.; Liu, Z.; Chen, Z.; Ren, Y.; Wang, S.; Zhang, X.; Wang, X. Enhanced heavy metal removal from an aqueous environment using an eco-friendly and sustainable adsorbent. *Sci. Rep.* **2020**, *10*, 16453. [[CrossRef](#)] [[PubMed](#)]
131. Liu, X.; Hu, Q.; Fang, Z.; Zhang, X.; Zhang, B. Magnetic Chitosan Nanocomposites: A Useful Recyclable Tool for Heavy Metal Ion Removal. *Langmuir* **2009**, *25*, 3–8. [[CrossRef](#)] [[PubMed](#)]
132. Chen, D.; Awut, T.; Liu, B.; Ma, Y.; Wang, T.; Nurulla, I. Functionalized magnetic Fe₃O₄ nanoparticles for removal of heavy metal ions from aqueous solutions. *e-Polymers* **2016**, *16*, 313–322. [[CrossRef](#)]
133. Huang, Z.-n.; Wang, X.-l.; Yang, D.-s. Adsorption of Cr(VI) in wastewater using magnetic multi-wall carbon nanotubes. *Water Sci. Eng.* **2015**, *8*, 226–232. [[CrossRef](#)]
134. Rivera, F.L.; Palomares, F.J.; Herrasti, P.; Mazario, E. Improvement in Heavy Metal Removal from Wastewater Using an External Magnetic Inductor. *Nanomaterials* **2019**, *9*, 1508. [[CrossRef](#)]
135. Tao, S.; Wang, C.; Ma, W.; Wu, S.; Meng, C. Designed multifunctionalized magnetic mesoporous microsphere for sequential sorption of organic and inorganic pollutants. *Microporous Mesoporous Mater.* **2012**, *147*, 295–301. [[CrossRef](#)]
136. Zheng, T.; Li, J.; Ji, Y.; Zhang, W.; Fang, Y.; Xin, F.; Dong, W.; Wei, P.; Ma, J.; Jiang, M. Progress and Prospects of Bioelectrochemical Systems: Electron Transfer and Its Applications in the Microbial Metabolism. *Front. Bioeng. Biotechnol.* **2020**, *8*, 10. [[CrossRef](#)]
137. Bajracharya, S.; Sharma, M.; Mohanakrishna, G.; Dominguez Benneton, X.; Strik, D.P.B.T.B.; Sarma, P.M.; Pant, D. An overview on emerging bioelectrochemical systems (BESs): Technology for sustainable electricity, waste remediation, resource recovery, chemical production and beyond. *Renew. Energy* **2016**, *98*, 153–170. [[CrossRef](#)]
138. Sukrampal; Kumar, R.; Patil, S.A. 3—Removal of heavy metals using bioelectrochemical systems. In *Integrated Microbial Fuel Cells for Wastewater Treatment*; Abbassi, R., Yadav, A.K., Khan, F., Garaniya, V., Eds.; Butterworth-Heinemann: Oxford, UK, 2020; pp. 49–71.
139. Rabaey, K.; Lissens, G.; Siciliano, S.D.; Verstraete, W. A microbial fuel cell capable of converting glucose to electricity at high rate and efficiency. *Biotechnol. Lett.* **2003**, *25*, 1531–1535. [[CrossRef](#)]

140. Kumar, R.; Yadav, S.; Patil, S.A. Bioanode-Assisted Removal of Hg^{2+} at the Cathode of Microbial Fuel Cells. *J. Hazard. Toxic Radioact. Waste* **2020**, *24*, 04020034. [\[CrossRef\]](#)
141. Zhang, Y.; Sun, J.; Hu, Y.; Li, S.; Xu, Q. Bio-cathode materials evaluation in microbial fuel cells: A comparison of graphite felt, carbon paper and stainless steel mesh materials. *Int. J. Hydrogen Energy* **2012**, *37*, 16935–16942. [\[CrossRef\]](#)
142. Yang, Q.; Liang, S.; Liu, J.; Lv, J.; Feng, Y. Analysis of Anodes of Microbial Fuel Cells When Carbon Brushes Are Preheated at Different Temperatures. *Catalysts* **2017**, *7*, 312. [\[CrossRef\]](#)
143. He, Y.-R.; Xiao, X.; Li, W.-W.; Sheng, G.-P.; Yan, F.-F.; Yu, H.-Q.; Yuan, H.; Wu, L.-J. Enhanced electricity production from microbial fuel cells with plasma-modified carbon paper anode. *Phys. Chem. Chem. Phys.* **2012**, *14*, 9966–9971. [\[CrossRef\]](#) [\[PubMed\]](#)
144. Ezziat, L.; Elabed, A.; Ibensouda, S.; El Abed, S. Challenges of Microbial Fuel Cell Architecture on Heavy Metal Recovery and Removal From Wastewater. *Front. Energy Res.* **2019**, *7*. [\[CrossRef\]](#)
145. Logan, B.; Cheng, S.; Watson, V.; Estadt, G. Graphite Fiber Brush Anodes for Increased Power Production in Air-Cathode Microbial Fuel Cells. *Environ. Sci. Technol.* **2007**, *41*, 3341–3346. [\[CrossRef\]](#)
146. Fan, Y.; Liu, H. *Materials for Low-Temperature Fuel Cells*; Wiley: Hoboken, NJ, USA, 2014; pp. 145–166.
147. Savla, N.; Anand, R.; Pandit, S.; Prasad, R. Utilization of Nanomaterials as Anode Modifiers for Improving Microbial Fuel Cells Performance. *J. Renew. Mater.* **2020**, *8*, 1581–1605. [\[CrossRef\]](#)
148. Nakamura, R.; Kai, F.; Okamoto, A.; Newton, G.J.; Hashimoto, K. Self-Constructed Electrically Conductive Bacterial Networks. *Angew. Chem. Int. Ed.* **2009**, *48*, 508–511. [\[CrossRef\]](#)
149. Zhao, C.; Wang, Y.; Shi, F.; Zhang, J.; Zhu, J.-J. High biocurrent generation in *Shewanella*-inoculated microbial fuel cells using ionic liquid functionalized graphene nanosheets as an anode. *Chem. Commun.* **2013**, *49*, 6668–6670. [\[CrossRef\]](#) [\[PubMed\]](#)
150. Zhao, C.; Gai, P.; Liu, C.; Wang, X.; Xu, H.; Zhang, J.; Zhu, J.-J. Polyaniline networks grown on graphene nanoribbons-coated carbon paper with a synergistic effect for high-performance microbial fuel cells. *J. Mater. Chem. A* **2013**, *1*, 12587. [\[CrossRef\]](#)
151. Hou, J.; Liu, Z.; Zhang, P. A new method for fabrication of graphene/polyaniline nanocomplex modified microbial fuel cell anodes. *J. Power Sources* **2013**, *224*, 139–144. [\[CrossRef\]](#)
152. Dessie, Y.; Tadesse, S.; Eswaramoorthy, R.; Adimasu, Y. Biosynthesized α - MnO_2 -based polyaniline binary composite as efficient bioanode catalyst for high-performance microbial fuel cell. *All Life* **2021**, *14*, 541–568. [\[CrossRef\]](#)
153. Mehdinia, A.; Ziaei, E.; Jabbari, A. Facile microwave-assisted synthesized reduced graphene oxide/tin oxide nanocomposite and using as anode material of microbial fuel cell to improve power generation. *Int. J. Hydrogen Energy* **2014**, *39*, 10724–10730. [\[CrossRef\]](#)
154. Velvizhi, G.; Venkata Mohan, S. Biocatalyst behavior under self-induced electrogenic microenvironment in comparison with anaerobic treatment: Evaluation with pharmaceutical wastewater for multi-pollutant removal. *Bioresour. Technol.* **2011**, *102*, 10784–10793. [\[CrossRef\]](#) [\[PubMed\]](#)
155. Tao, C.-H.; Liang, M.; Li, W.; Zhang, J.-L.; Ni, R.-J.; Wu, M.-W. Removal of copper from aqueous solution by electrodeposition in cathode chamber of microbial fuel cell. *J. Hazard. Mater.* **2011**, *189*, 186–192. [\[CrossRef\]](#)
156. Huang, L.; Chen, J.; Quan, X.; Yang, F. Enhancement of hexavalent chromium reduction and electricity production from a biocathode microbial fuel cell. *Bioprocess. Biosyst. Eng.* **2010**, *33*, 937–945. [\[CrossRef\]](#) [\[PubMed\]](#)
157. Zhang, B.; Feng, C.; Ni, J.; Zhang, J.; Huang, W. Simultaneous reduction of vanadium (V) and chromium (VI) with enhanced energy recovery based on microbial fuel cell technology. *J. Power Sources* **2012**, *204*, 34–39. [\[CrossRef\]](#)
158. Wang, G.; Huang, L.; Zhang, Y. Cathodic reduction of hexavalent chromium [Cr(VI)] coupled with electricity generation in microbial fuel cells. *Biotechnol. Lett.* **2008**, *30*, 1959. [\[CrossRef\]](#) [\[PubMed\]](#)
159. Wang, Z.; Lim, B.; Choi, C. Removal of Hg^{2+} as an electron acceptor coupled with power generation using a microbial fuel cell. *Bioresour. Technol.* **2011**, *102*, 6304–6307. [\[CrossRef\]](#)
160. Rodenas Motos, P.; ter Heijne, A.; van der Weijden, R.; Saakes, M.; Buisman, C.J.N.; Sleutels, T.H.J.A. High rate copper and energy recovery in microbial fuel cells. *Front. Microbiol.* **2015**, *6*, 527. [\[CrossRef\]](#) [\[PubMed\]](#)
161. Choi, C.; Cui, Y. Recovery of silver from wastewater coupled with power generation using a microbial fuel cell. *Bioresour. Technol.* **2012**, *107*, 522–525. [\[CrossRef\]](#) [\[PubMed\]](#)
162. Catal, T.; Bermek, H.; Liu, H. Removal of selenite from wastewater using microbial fuel cells. *Biotechnol. Lett.* **2009**, *31*, 1211–1216. [\[CrossRef\]](#) [\[PubMed\]](#)
163. Huang, L.; Li, T.; Liu, C.; Quan, X.; Chen, L.; Wang, A.; Chen, G. Synergetic interactions improve cobalt leaching from lithium cobalt oxide in microbial fuel cells. *Bioresour. Technol.* **2013**, *128*, 539–546. [\[CrossRef\]](#) [\[PubMed\]](#)
164. Lim, B.S.; Lu, H.; Choi, C.; Liu, Z.X. Recovery of silver metal and electric power generation using a microbial fuel cell. *Desalination Water Treat.* **2015**, *54*, 3675–3681. [\[CrossRef\]](#)
165. Gupta, S.; Yadav, A.; Verma, N. Simultaneous Cr(VI) reduction and bioelectricity generation using microbial fuel cell based on alumina-nickel nanoparticles-dispersed carbon nanofiber electrode. *Chem. Eng. J.* **2017**, *307*, 729–738. [\[CrossRef\]](#)
166. Shi, J.; Zhao, W.; Liu, C.; Jiang, T.; Ding, H. Enhanced Performance for Treatment of Cr (VI)-Containing Wastewater by Microbial Fuel Cells with Natural Pyrrhotite-Coated Cathode. *Water* **2017**, *9*, 979. [\[CrossRef\]](#)
167. Wu, Y.; Wang, L.; Jin, M.; Kong, F.; Qi, H.; Nan, J. Reduced graphene oxide and biofilms as cathode catalysts to enhance energy and metal recovery in microbial fuel cell. *Bioresour. Technol.* **2019**, *283*, 129–137. [\[CrossRef\]](#) [\[PubMed\]](#)
168. Li, M.; Zhou, S. α - Fe_2O_3 /polyaniline nanocomposites as an effective catalyst for improving the electrochemical performance of microbial fuel cell. *Chem. Eng. J.* **2018**, *339*, 539–546. [\[CrossRef\]](#)

-
169. Ali, J.; Wang, L.; Waseem, H.; Djellabi, R.; Oladoja, N.A.; Pan, G. FeS@rGO nanocomposites as electrocatalysts for enhanced chromium removal and clean energy generation by microbial fuel cell. *Chem. Eng. J.* **2020**, *384*, 123335. [[CrossRef](#)]
 170. Xue, A.; Shen, Z.-Z.; Zhao, B.; Zhao, H.-Z. Arsenite removal from aqueous solution by a microbial fuel cell–zerovalent iron hybrid process. *J. Hazard. Mater.* **2013**, *261*, 621–627. [[CrossRef](#)] [[PubMed](#)]
 171. Qin, B.; Luo, H.; Liu, G.; Zhang, R.; Chen, S.; Hou, Y.; Luo, Y. Nickel ion removal from wastewater using the microbial electrolysis cell. *Bioresour. Technol.* **2012**, *121*, 458–461. [[CrossRef](#)] [[PubMed](#)]
 172. Choi, C.; Hu, N.; Lim, B. Cadmium recovery by coupling double microbial fuel cells. *Bioresour. Technol.* **2014**, *170*, 361–369. [[CrossRef](#)] [[PubMed](#)]
 173. Ge, Z.; Li, J.; Xiao, L.; Tong, Y.; He, Z. Recovery of Electrical Energy in Microbial Fuel Cells. *Environ. Sci. Technol. Lett.* **2014**, *1*, 137–141. [[CrossRef](#)]
 174. Fan, Y.; Hu, H.; Liu, H. Enhanced Coulombic efficiency and power density of air-cathode microbial fuel cells with an improved cell configuration. *J. Power Sources* **2007**, *171*, 348–354. [[CrossRef](#)]
 175. Liu, H.; Cheng, S.; Logan, B.E. Production of Electricity from Acetate or Butyrate Using a Single-Chamber Microbial Fuel Cell. *Environ. Sci. Technol.* **2005**, *39*, 658–662. [[CrossRef](#)] [[PubMed](#)]
 176. Tang, X.; Guo, K.; Li, H.; Du, Z.; Tian, J. Microfiltration membrane performance in two-chamber microbial fuel cells. *Biochem. Eng. J.* **2010**, *52*, 194–198. [[CrossRef](#)]